JOURNAL OF GEOPHYSICAL RESEARCH, VOL. 90, NO. D7, PAGES 12,999–13,029, DECEMBER 20, 1985

A Critical Analysis of CLO and 0_3 in the Mid-Latitude Stratosphere

LUCIEN FROIDEVAUX,[1] MARK ALLEN,[1] AND YUK L. YUNG

Division of Geological and Planetary Sciences, California Institute of Technology, Pasadena.

In the upper stratosphere, an altitude range in which ozone should be in photochemical steady-state, calculated ozone abundances that are derived from a one-dimensional photochemical model with updated chemistry are up to 60% smaller than mean observed values. On the other hand, the model results for the key free radicals (HO_x, NO_x, and ClO_x species) in the catalytic destruction of ozone are shown to be in reasonable agreement with available measurements. The general validity of the model simulation of ClO_x chemistry is confirmed through a detailed intercomparison between the computed ClO diurnal variation and recently published ground-based microwave observations. Since many field measurements are performed near sunrise or sunset, the uncertainties in the model results arising from the details of the radiation field calculations at large zenith angles are discussed. Although the calculated ozone discrepancy could be the result of a number of errors in adopted photochemical parameters, a sensitivity analysis shows that no reasonable change in any one or two parameters can resolve this problem. The limited available observations regarding the ratio of atomic oxygen to ozone suggest a possible discrepancy in that quantity, which could be responsible for a large part of the ozone problem.

1. INTRODUCTION

The mean values of the measured abundances of minor and trace gases observed in the terrestrial stratosphere to date are reproduced reasonably well by models of photochemistry and dynamics of this region. In other words the combined knowledge of various chemical reaction rate constants and molecular absorption cross sections from laboratory experiments, solar fluxes above the earth's atmosphere from rocket and satellite measurements, and global transport processes from semiempirical analyses does yield a set of stratospheric species concentrations close to most in situ and remote sensing observations. However, certain significant discrepancies still remain or have recently emerged upon the updating of model parameters. This is a critical issue, since a more refined understanding of the stratosphere is needed for accurate predictions of the effects of perturbations due to man. Of prime importance is the possibly irreversible depletion of the ozone layer as a consequence of stratospheric photolysis of anthropogenically produced halocarbons [*Molina and Rowland*, 1974; *Rowland and Molina*, 1975], although the impact of a small (10%) decrease in total column ozone on humans and animals (sunburn, effects on DNA and immune system response, skin cancer) as well as plants is not yet well defined [*National Research Council*, 1982]. *Cicerone et al.* [1983] and *Prather et al.* [1984] have recently pointed out some of the nonlinearities involved in the photochemistry alone. Ozone changes, however, could also influence the radiative forcing of atmospheric motions and--ultimately--the global climate. Predictions of ozone depletion over the next century have varied not only in magnitude but also in sign. This is due to our uncertain, and maybe yet incomplete, understanding of the present stratospheric photochemistry, which is closely coupled to refinements in relevant laboratory data and measurements of key species.

In this paper we use the Caltech one-dimensional photochemical model to analyze important questions concerning upper stratospheric O_3 and the key HO_x, NO_x, and ClO_x free radicals. Applications of the basic model to mesospheric and thermospheric photochemistry have been discussed by *Allen et al.* [1981, 1984]. A brief description of the stratospheric model was presented by *Froidevaux and Yung* [1982] in relation to the sensitivity of certain vertical profiles ($CFCl_3$ in particular) to O_2 absorption cross sections in the Herzberg continuum. The growing number of two-dimensional models of the stratosphere is an indication that the latitudinal and seasonal trends in species concentrations can now be more realistically modeled but also that the available data coverage--from space in particular--is becoming increasingly global. Nevertheless there will always be a class of scientific questions that can be analyzed with a simple one-dimensional approach and without the need for more expensive and time-consuming treatments. In particular, if several chemically long-lived species are detected by a given experiment (or maybe prescribed by a multidimensional model), their concentrations can be used as fixed inputs for a one-dimensional model, which can then be used to study the abundances of short-lived (reactive) species as a function of altitude and time of day. Moreover, in the upper stratosphere, O_3 is only indirectly affected by transport processes. Therefore one-dimensional O_3 calculations in this region are valid if the profiles of the long-lived species and derivative free radicals are close to observed values. In this case the one-dimensional model provides a very economical mode for analyzing the sensitivity of the O_3 results to adopted model parameters.

The basic stratospheric model is described in section 2. Because of the existence of numerous observations taken during sunrise or sunset, we assess, in subsection 2.2, the first-order effects (on the calculated chemical abundances) of the inclusion of diffuse (Rayleigh scattered) radiation in a spherical-rather than plane parallel-atmosphere at solar zenith angles close to 90°. The most important problem dis-

[1] Now at Jet Propulsion Laboratory, California Institute of Technology, Pasadena.

Paper number 5D0467.
0148-0227/85/005D-0467$05.00

cussed below concerns the present stratospheric abundance of ozone, a question that, in our view, has been somewhat neglected in favor of calculations of potential (but rather uncertain) amounts of future ozone depletion. We focus in section 5 on this comparison between photochemical theory and observations for upper stratospheric ozone, where local photochemistry rather than dynamics should control the O_3 abundance. The relevant photochemical equilibrium relation for odd oxygen ($O_x = O + O_3$) involves production by photodissociation of O_2 and destruction by direct recombination between O and O_3 as well as important catalytic cycles due to reactions with radicals of HO_x (OH, HO_2), NO_x (NO, NO_2), and ClO_x (Cl, ClO). An analysis of this balance should therefore also include a comparison between observations of these important radicals and corresponding model results. We discuss HO_x and NO_x observations in section 3, while section 4 deals with chlorine chemistry. In light of recent ground-based measurements of diurnal changes in ClO [*Solomon et al.*, 1984] and other relevant data we analyze the diurnal variation of this key radical in subsection 4.2. Given the decreasing uncertainties in laboratory data (reaction rate constants and absorption cross sections) and the available data on key radical concentrations, we are led to conclude, in section 5, that there exists a significant model ozone deficit in the upper stratosphere. We investigate possible causes for such a discrepancy in light of current model and experimental uncertainties. In particular the observational ratio of atomic oxygen to ozone appears to disagree with our model results. Since few model parameters affect this ratio, a confirmation of this result by additional measurements may help resolve the apparent ozone discrepancy. Further details regarding parts of this paper may be found in *Froidevaux* [1983].

2. The Caltech Photochemical Model

2.1. *Basic Description*

The results reported in this paper were obtained from a photochemical model that solves the continuity equation for each species in a one-dimensional (vertical) system, and transport is parametrized in the standard eddy diffusion formulation [see *Allen et al.*, 1981; *Froidevaux*, 1983]. Once a steady state diurnal average solution has been found, source species that are long-lived with respect to transport processes can be fixed. A diurnal calculation is then performed for other species, and no transport is involved. Such decoupling of transport and photochemistry allows for a more economical solution to be reached in the diurnal case. Another feature of the model involves the implementation of spherical geometry. Sphericity is accounted for in the flux divergence term, in the varying daylight period as a function of altitude, as well as in the calculation of slant optical depths.

After experimenting with various types of boundary conditions, we conclude that, in general, our results at altitudes sufficiently removed (5-10 km) from the boundaries are relatively insensitive to the adopted boundary conditions. The only exceptions to this statement are the bottom boundary conditions for the source species that diffuse upward into the stratosphere and directly affect the photochemistry of that region; these are N_2O, CH_4, the halocarbons, and H_2O. For the four major halocarbons the mixing ratios

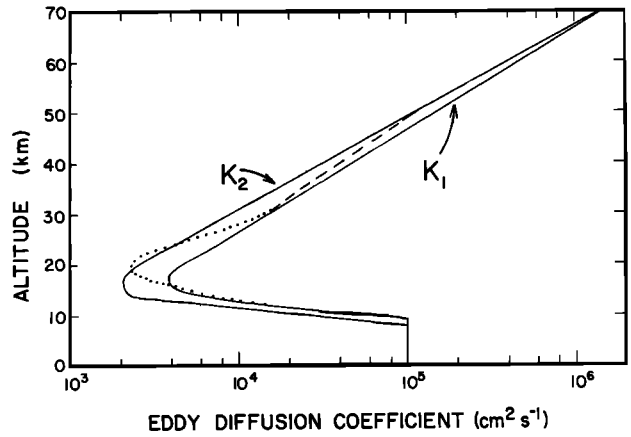

Fig. 1. Model eddy diffusion profiles versus height. Profile K_1 is very similar to the composite profile (dashed line) deduced by *Massie and Hunten* [1981], the two profiles being identical below 30 km, and is used for latitudes near 30°N. Profile K_2 is preferred for latitudes near 45°N (see text) and has a lower-stratospheric minimum value that is close to the value derived from $^{14}CO_2$ tracer data by Massie and Hunten (dotted line).

prescribed at the surface of the earth correspond to average 1978 values: 0.24 ppb for CF_2Cl_2, 0.14 ppb for $CFCl_3$, 0.13 ppb for CCl_4, and 0.61 ppb for $C_2H_3Cl_3$. Boundary conditions for FC113 (19 ppt) and FC114 (12 ppt) are taken from the review by *Cicerone* [1981], and the FC22 value is consistent with measurements of *Rasmussen et al.* [1982] and *Leifer et al.* [1981], which indicate about 50 ppt (slightly less than our adopted value of 60 ppt) near the ground at northern mid-latitudes. The N_2O and CH_4 values are 0.31 ppm and 1.65 ppm, respectively. When the lower boundary of the calculations is at 16 km, the boundary condition for H_2O is set at 3.6 ppm. Additional details on our choice of boundary conditions may be found in *Froidevaux* [1983].

The eddy diffusion coefficients used in this work were described in *Froidevaux and Yung* [1982] and are plotted in Figure 1. We have varied the eddy diffusion profile in various ways and checked the sensitivity of N_2O, CH_4, and halocarbon mid-latitude profiles to transport. Given the range of observed profiles, there is no unique solution for an acceptable eddy diffusion profile, although it is clear that a sharp decrease in the lower stratosphere (~18 km), followed by a relatively smooth increase to higher altitudes, is needed. If the increase is too abrupt, values of N_2O, CH_4, and chlorofluorocarbon mixing ratios become too large compared to observations. As discussed in Froidevaux and Yung, the sharp decrease in the abundance of halocarbons (FC11 in particular) in the stratosphere probably requires more than a vertical transport adjustment (in order to still fit N_2O and CH_4 observations), and the implication is that the radiation field near 200 nm should also be accurately determined. The "best fit" composite eddy diffusion profile of *Massie and Hunten* [1981], along with their $^{14}CO_2$ profile, is shown in Figure 1 (0-50 km). Our profile $K_1(z)$ is very similar to the composite profile and is continued upward to 70 km, where it matches the $K(z)$ value obtained by *Allen et al.* [1981] in a study of O, O_2, CO_2, Ar, and CO observations in relation to thermospheric and mesospheric transport. This profile is used (in conjunction with the values above 70 km from *Allen et al.* [1981] for our stan-

dard models near 30°N. For observations of N_2O, CF_2Cl_2, and $CFCl_3$ near 45°N [see *Hudson et al.*, 1982] we prefer to use a somewhat slower rate of mixing, namely profile $K_2(z)$ in Figure 1. It is generally agreed that vertical transport decreases from the equatorial regions (upwelling part of Hadley cell) to mid-latitudes. This idea seems to be supported by observations of the mixing ratio vertical gradients for CH_4 [*Ehhalt and Tonnissen*, 1980] as a function of latitude, as well as for N_2O, CF_2Cl_2, $CFCl_3$, and CCl_4 [*Vedder et al.*, 1978, 1981; *Goldan et al.*, 1980; *Gallagher et al.*, 1983].

Table 1*a* lists the set of chemical reactions used here and the associated rate constants (two-body, three-body, or equilibrium constants). The chemical reactions in Table 1*a* will be referred to as (R1) through (R110). Since our model spans the 0-80 km range, some of these reactions are more important in the troposphere or mesosphere than in the stratosphere directly but are included in order to minimize uncertainties in fluxes to the stratosphere or in boundary effects. The set of reaction rate constants is mostly taken from *DeMore et al.* [1982]. It is worth noting that only a few minor changes have been recommended in the latest kinetic data evaluation [see *DeMore et al.*, 1983]. Many rate constants now seem to be well constrained by several laboratory experiments, often using different techniques. At room temperature the uncertainty in most of the important reaction rate constants is about 10%-25%. This is often true at the colder stratospheric temperatures as well. However, reactions with a strong temperature dependence (O + O_3, for example) can suffer from larger uncertainties.

The rate constants for the various channels of the H + HO_2 reactions (k_{23}, k_{24}, and k_{25}), are consistent with the experimental results of *Sridharan et al.* [1982]. The expression used for H_2O_2 formation, (R26), is based on the work of *Kircher and Sander* [1984] (S. Sander, private communication, 1982), without their more recently determined temperature dependence

$$k_{26} = \frac{k_o + 5.2 \times 10^{-11}\mathrm{C(H_2O)} + 1.2 \times 10^{-14}[\mathrm{C(H_2O)}]^2}{[1 + \mathrm{C(H_2O)}]^2} \times (1 + 5.4 \times 10^{-32}\,[M] / k_o) \quad (1)$$

where $k_o = 4.5 \times 10^{-14}\, e^{1200/T}$ and $\mathrm{C(H_2O)} = 1.25 \times 10^{-25}\, e^{4100/T}\,[\mathrm{H_2O}]$. The bracketed term includes a water-vapor-dependent effect (useful only in the troposphere) and its associated temperature dependence, whereas the second term expresses the pressure-dependent effect. The value of k_{26} should be about 40% lower than if calculated by using (1), according to the temperature-dependent results of *Kircher and Sander* [1984], *Patrick and Pilling* [1982], and *Thrush and Tyndall* [1982]. The latest kinetic data evaluation [*DeMore et al.*, 1983] gives a recommendation consistent with these studies, whose main effect is to lower the calculated H_2O_2 stratospheric abundance. The OH + HO_2 reaction rate constant (k_{29}) follows the pressure dependence recommended in *DeMore et al.* [1982] but includes a temperature-dependent factor consistent with the results of *Kaufman et al.* [1982] and increases the calculated total HO_x (OH + HO_2) destruction rate by 10%-40% in the stratosphere. Their final published value [*Sridharan et al.*, 1984] is only slightly different than our adopted value (at low pressures).

The HO_2NO_2 formation reaction rate constant k_{47} is slightly modified to account for tropospheric water vapor dependence [*Sander and Peterson*, 1984], which introduces a multiplicative factor of $(1 + 1.07 \times 10^{-18}\,[\mathrm{H_2O}])$. Recent determinations of the rate constants k_{55} and k_{60} for the O + *Cl*O and OH + HC*l* reactions are discussed later in this paper. The rate constant k_{66} used for $ClONO_2$ formation follows the "fast" recommended value in *DeMore et al.* [1982] and is consistent with chlorine nitrate being "the sole product of the *Cl*O + NO_2 + M recombination," as demonstrated by *Margitan* [1983]. The equilibrium rate constant used in the expression for k_{86} was obtained by S. Sander (private communication, 1982) from data on the thermal decomposition of $CH_3O_2NO_2$ [*Bahta et al.*, 1982], coupled with the forward rate constant data of *Sander and Watson* [1980]. We note that the rate constant for reaction (R88) between OH and C_2H_2 should be modified at low pressures for best comparison with stratospheric C_2H_2 data [see *DeMore et al.*, 1983, for full expression].

Reaction (R101) schematically represents the average latitude-dependent production of NO by cosmic ray ionization of nitrogen, mostly in the lower stratosphere [see *Dalgarno*, 1967; *Nicolet*, 1975b]. This source varies with solar activity (deflecting action) and latitude (magnetic focusing at high latitudes), and we have used average production rates based on *Nicolet* [1975b] for six latitude bins (four 10° bins between 15° and 55°, one bin below 15°, and one above 55°). This produces a nonnegligible natural source of NO mostly at high latitudes and at night [see also *Ashby*, 1976]. Reaction (R102) represents a tropospheric source of odd nitrogen apparently required (in simple one-dimensional models) to match observations of NO_x, HNO_3, and O_3 in the clean troposphere [see *Logan et al.*, 1981]. Lightning and oxidation of ammonia have been proposed as significant global odd nitrogen sources, but the relative role of in situ sources versus downward transport from the stratosphere is not yet well determined in terms of NO_x and O_3 production in the troposphere [see, for example, *Fishman and Crutzen*, 1977; *Fishman*, 1981; *Callis et al.*, 1983; *Liu et al.*, 1983]. Finally, reactions (R103) through (R110) are an attempt to describe average rainout losses for water soluble gases in the troposphere, as discussed in *Logan et al.* [1981].

The molecular photoreactions and associated absorption cross section references for the relevant wavelength ranges are listed in Table 1*b*. These reactions will be referred to as (J1) through (J35). Also shown in this table are the calculated photodissociation rate constants (s^{-1}), including Rayleigh scattering (as explained below), for a solar zenith angle of 45° at altitudes of 40 and 20 km. Our total coverage in wavelength extends from 96 to 800 nm. Reactions (J1) through (J4), (J34), and (J35) constitute the important processes that contribute to the atmospheric opacity. Reaction (J34) represents absorption by NO_2 without dissociation (as opposed to NO_2 photolysis in reaction (J9)) and is generally quite small compared to absorption by O_2 or O_3. Reaction (J35) refers to the Rayleigh scattering cross sections and their effect on the attenuation of the direct flux. From 175 to 200 nm we have to deal with the very fine structure of the O_2 Schumann-Runge bands [see also,

TABLE 1*a*. Chemical Reactions

	Reaction	Rate Constant*	Reference†
(1)	$O + O_2 + M \rightarrow O_3 + M$	(3.0(-28) $T^{-2.3}$; 2.8(-12); 0.85)	*Baulch et al.* [1982]
(2)	$O + O_3 \rightarrow 2O_2$	1.5(-11) $e^{-2218/T}$	
(3)	$2O + M \rightarrow O_2 + M$	4.3(-28) $T^{-2.0}$	*Hampson* [1980]
(4)	$O(^1D) + O_2 \rightarrow O + O_2$	3.2(-11) $e^{67/T}$	
(5)	$O(^1D) + N_2 \rightarrow O + N_2$	1.8(-11) $e^{107/T}$	
(6)	$O(^1D) + H_2 \rightarrow 2OH$	2.2(-10)	
(7)	$O(^1D) + H_2 \rightarrow H + OH$	1.0(-10)	
(8)	$O(^1D) + CH_4 \rightarrow CH_3 + OH$	1.4(-10)	
(9)	$O(^1D) + CH_4 \rightarrow H_2 + H_2CO$	1.4(-11)	
(10)	$O(^1D) + N_2O \rightarrow 2NO$	6.7(-11)	
(11)	$O(^1D) + N_2O \rightarrow N_2 + O_2$	4.9(-11)	
(12)	$O(^1D) + CFCl_3 \rightarrow 3Cl$ + products	2.3(-10)	
(13)	$O(^1D) + CF_2Cl_2 \rightarrow 2Cl$ + products	1.4(-10)	
(14)	$CHF_2Cl + O(^1D) \rightarrow HCl$ + products	1.9(-10)	*Pitts et al.* [1974]
(15)	$C_2F_3Cl_3 + O(^1D) \rightarrow 3Cl$ + products	2.9(-10)	*Pitts et al.* [1974]
(16)	$C_2F_4Cl_2 + O(^1D) \rightarrow 2Cl$ + products	1.8(-10)	*Pitts et al.* [1974]
(17)	$O + OH \rightarrow O_2 + H$	2.2(-11) $e^{117/T}$	
(18)	$O + HO_2 \rightarrow OH + O_2$	3.0(-11) $e^{200/T}$	
(19)	$OH + O_3 \rightarrow HO_2 + O_2$	1.6(-12) $e^{-940/T}$	
(20)	$HO_2 + O_3 \rightarrow OH + 2O_2$	1.4(-14) $e^{-580/T}$	
(21)	$H + O_2 + M \rightarrow HO_2 + M$	1.6(-28) $T^{-1.4}$	
(22)	$H + O_3 \rightarrow OH + O_2$	1.4(-10) $e^{-470/T}$	
(23)	$H + HO_2 \rightarrow H_2 + O_2$	3.8(-12)	see text
(24)	$H + HO_2 \rightarrow 2OH$	6.8(-11)	see text
(25)	$H + HO_2 \rightarrow H_2O + O$	3.2(-12)	see text
(26)	$2HO_2 \rightarrow H_2O_2 + O_2$		see text
(27)	$2OH + M \rightarrow H_2O_2 + M$	(2.1(-28) $T^{-1.0}$; 3.0(-9) $T^{-1.0}$; 0.6)	
(28)	$H_2O_2 + OH \rightarrow H_2O + HO_2$	3.1(-12) $e^{-187/T}$	
(29)	$OH + HO_2 \rightarrow H_2O + O_2$	2.2(-12) exp(450/T)[7 + 4 P]	see text
(30)	$H_2 + OH \rightarrow H_2O + H$	6.1(-12) $e^{2030/T}$	
(31)	$2OH \rightarrow H_2O + O$	4.2(-12) $e^{-242/T}$	
(32)	$O + NO_2 \rightarrow NO + O_2$	9.3(-12)	
(33)	$O_3 + NO \rightarrow NO_2 + O_2$	2.2(-12) $e^{-1430/T}$	
(34)	$HO_2 + NO \rightarrow NO_2 + OH$	3.7(-12) $e^{240/T}$	
(35)	$NO + O + M \rightarrow NO_2 + M$	(3.5(-27) $T^{-1.8}$; 3.0(-11); 0.6)	
(36)	$NO_2 + O_3 \rightarrow NO_3 + O_2$	1.2(-13) $e^{-2450/T}$	
(37)	$NO_2 + O + M \rightarrow NO_3 + M$	(8.1(-27) $T^{-2.0}$; 2.2(-11); 0.6)	
(38)	$NO_3 + NO \rightarrow 2NO_2$	2.0(-11)	
(39)	$O + NO_3 \rightarrow O_2 + NO_2$	1.0(-11)	
(40)	$NO_3 + NO_2 + M \rightarrow N_2O_5 + M$	(1.9(-23) $T^{-2.8}$; 1.0(-12); 0.6)	
(41)	$N_2O_5 + M \rightarrow NO_3 + NO_2 + M$	k_{40}/(1.77(-27) $e^{11001/T}$)	
(42)	$N + O_3 \rightarrow NO + O_2$	1.0(-15)	
(43)	$N + O_2 \rightarrow NO + O$	4.4(-12) $e^{-3220/T}$	
(44)	$N + NO \rightarrow N_2 + O$	3.4(-11)	
(45)	$OH + NO_2 + M \rightarrow HNO_3 + M$	(4.0(-23) $T^{-2.9}$; 4.0(-8) $T^{-1.3}$; 0.6)	
(46)	$OH + HNO_3 \rightarrow NO_3 + H_2$	9.4(-15) $e^{778/T}$	

TABLE 1*a*. Chemical Reactions

	Reaction	Rate Constant*	Reference†
(47)	$HO_2 + NO_2 + M \rightarrow HO_2NO_2 + M$	(5.7(-20) $T^{-4.6}$; 4.2(-12); 0.6)	
(48)	$HO_2NO_2 + OH \rightarrow H_2O + NO_2 + O_2$	1.3(-12) $e^{380/T}$	
(49)	$HO_2NO_2 + M \rightarrow HO_2 + NO_2 + M$	k_{47}/(2.33(-27) $e^{10870/T}$)	
(50)	$OH + NO + M \rightarrow HNO_2 + M$	(1.0(-24) $T^{-2.5}$; 2.6(-10) $T^{-0.5}$; 0.6)	
(51)	$NO + CH_3O_2 \rightarrow HNO_2 + H_2CO$	7.4(-13) (10% of k_{73})	
(52)	$HO_2 + NO_2 \rightarrow HNO_2 + O_2$	3.0(-15)	*Hampson and Garvin* [1978]
(53)	$OH + HNO_2 \rightarrow H_2O + NO_2$	6.6(-12)	
(54)	$Cl + O_3 \rightarrow ClO + O_2$	2.8(-11) $e^{-257/T}$	
(55)	$O + ClO \rightarrow Cl + O_2$	7.7(-11) $e^{-130/T}$	see text
(56)	$ClO + NO \rightarrow Cl + NO_2$	6.2(-12) $e^{294/T}$	
(57)	$ClO + OH \rightarrow HO_2 + Cl$	5.1(-12) $e^{180/T}$	
(58)	$Cl + O_2 + M \rightarrow ClOO + M$	3.3(-30) $T^{-1.3}$	
(59)	$ClOO + M \rightarrow Cl + O_2 + M$	k_{58}/(2.43(-25) $e^{2979/T}$)	
(60)	$OH + HCl \rightarrow Cl + H_2O$	2.8(-12) $e^{-425/T}$	see text
(61)	$Cl + CH_4 \rightarrow HCl + CH_3$	9.6(-12) $e^{-1350/T}$	
(62)	$Cl + HO_2 \rightarrow HCl + O_2$	1.8(-11) $e^{170/T}$	
(63)	$Cl + H_2 \rightarrow HCl + H$	3.7(-11) $e^{-2300/T}$	
(64)	$Cl + H_2CO \rightarrow HCl + HCO$	8.2(-11) $e^{-34/T}$	
(65)	$Cl + H_2O_2 \rightarrow HCl + HO_2$	1.1(-11) $e^{-980/T}$	
(66)	$ClO + NO_2 + M \rightarrow ClONO_2 + M$	(4.8(-23) $T^{-3.4}$; 7.6(-7) $T^{-1.9}$; 0.6)	see text
(67)	$ClONO_2 + O \rightarrow ClO + NO_3$	3.0(-12) $e^{-808/T}$	
(68)	$ClO + HO_2 \rightarrow HOCl + O_2$	4.6(-13) $e^{710/T}$	
(69)	$OH + HOCl \rightarrow H_2O + ClO$	3.0(-12) $e^{-150/T}$	
(70)	$CH_3Cl + OH \rightarrow Cl + H_2O$ + products	1.8(-12) $e^{-1112/T}$	
(71)	$C_2H_3Cl_3 + OH \rightarrow 3Cl$ + products	5.4(-12) $e^{-1820/T}$	
(72)	$CHF_2Cl + OH \rightarrow Cl$ + products	7.8(-13) $e^{-1530/T}$	
(73)	$OH + CH_4 \rightarrow CH_3 + H_2O$	2.4(-12) $e^{-1710/T}$	
(74)	$CH_3 + O_2 + M \rightarrow CH_3O_2 + M$	(6.2(-26) $T^{-2.2}$; 3.3(-8) $T^{-1.7}$; 0.6)	
(75)	$CH_3O_2 + NO \rightarrow CH_3O + NO_2$	4.2(-12) $e^{180/T}$	
(76)	$2CH_3O_2 \rightarrow 2CH_3O + O_2$	1.6(-13) $e^{220/T}$	
(77)	$CH_3O + O_2 \rightarrow H_2CO + HO_2$	1.2(-13) $e^{-1350/T}$	
(78)	$CH_3 + O_2 \rightarrow H_2CO + OH$	5.0(-17)	*Baulch et al.* [1982]
(79)	$CH_3 + O \rightarrow H_2CO + H$	1.4(-10)	
(80)	$H_2CO + OH \rightarrow HCO + H_2O$	1.0(-11)	
(81)	$H_2CO + O \rightarrow OH + HCO$	3.0(-11) $e^{-1550/T}$	
(82)	$HCO + O_2 \rightarrow CO + HO_2$	3.5(-12) $e^{140/T}$	
(83)	$CH_3O_2 + HO_2 \rightarrow CH_3OOH + O_2$	7.7(-14) $e^{1300/T}$	
(84)	$CH_3OOH + OH \rightarrow CH_3O_2 + H_2O$	2.6(-12) $e^{-190/T}$	
(85)	$CH_3O_2 + NO_2 + M \rightarrow CH_3O_2NO_2 + M$	(1.2(-20) $T^{-4.0}$; 5.8(-7) $T^{-2.0}$; 0.4)	F_c from *Baulch et al.* [1982]
(86)	$CH_3O_2NO_2 + M \rightarrow CH_3O_2 + NO_2 + M$	k_{85}/(1.2(-28) $e^{11320/T}$)	see text
(87)	$CO + OH \rightarrow CO_2 + H$	1.35(-13)[1 + P]	
(88)	$C_2H_2 + OH \rightarrow H_2$ + products	6.5(-12) $e^{-650/T}$	see text
(89)	$C_2H_6 + OH \rightarrow H_2O$ + products	1.9(-11) $e^{-1260/T}$	
(90)	$C_2H_6 + Cl \rightarrow HCl$ + products	7.7(-11) $e^{-90/T}$	
(91)	$C_3H_8 + OH \rightarrow H_2O$ + products	1.6(-11) $e^{-800/T}$	
(92)	$C_3H_8 + Cl \rightarrow HCl$ + products	1.4(-10) $e^{40/T}$	

TABLE 1*a*. Chemical Reactions

	Reaction	Rate Constant*	Reference†
(93)	$F + O_3 \rightarrow FO + O_2$	$2.8(-11)\, e^{-226/T}$	
(94)	$FO + NO \rightarrow F + NO_2$	2.6(-11)	
(95)	$2FO \rightarrow 2F + O_2$	1.5(-11)	
(96)	$FO + O \rightarrow F + O_2$	5.0(-11)	
(97)	$F + H_2O \rightarrow HF + OH$	$2.2(-11)\, e^{-200/T}$	
(98)	$F + CH_4 \rightarrow HF + CH_3$	$3.0(-10)\, e^{-400/T}$	
(99)	$F + H_2 \rightarrow HF + H$	$1.9(-10)\, e^{-570/T}$	
(100)	$HF + O(^1D) \rightarrow F + OH$	2.0(-10)	estimate
(101)	cosmic ray source $\rightarrow$ NO		*Nicolet* [1975b]
(102)	tropospheric source $\rightarrow NO_2$		*Logan et al.* [1981]
(103)	$H_2O_2 \xrightarrow{\text{rainout}}$ products		*Logan et al.* [1981]
(104)	$HNO_3 \xrightarrow{\text{rainout}}$ products		*Logan et al.* [1981]
(105)	$HO_2NO_2 \xrightarrow{\text{rainout}}$ products		*Logan et al.* [1981]
(106)	$HNO_2 \xrightarrow{\text{rainout}}$ products		*Logan et al.* [1981]
(107)	$HCl \xrightarrow{\text{rainout}}$ products		*Logan et al.* [1981]
(108)	$H_2CO \xrightarrow{\text{rainout}}$ products		*Logan et al.* [1981]
(109)	$CH_3OOH \xrightarrow{\text{rainout}}$ products		*Logan et al.* [1981]
(110)	$HF \xrightarrow{\text{rainout}}$ products		*Logan et al.* [1981]

* Read $a(-b)$ as $a \times 10^{-b}$. Units are $cm^3\ s^{-1}$ for two-body reactions. When a third body (M) is involved, the units for $k(M, T)$ are $cm^6\ s^{-1}$, and values are listed as (k_o; k_∞; F_c), where k_o ($cm^6\ s^{-1}$) and k_∞ ($cm^3\ s^{-1}$) are temperature-dependent low- and high-pressure limits. The expression for k is then written as

$$k = \frac{k_o[M]}{1 + (k_o[M]/k_\infty)} F_c^{\{1 + [\log (k_o [M]/k_\infty)]^2\}^{-1}}$$

In the above table, temperature (T) is expressed in degrees Kelvin and pressure (P) in atmospheres.

† Unless otherwise stated, reference is *DeMore et al.* [1982].

Frederick and Hudson, 1979, 1980; *Yoshino et al.*, 1983]. The computationally accurate (compared to line-by-line calculations) and efficient parametrization of altitude- and zenith-dependent O_2 cross sections by *Allen and Frederick* [1982] is used in this work. This also affects photolysis of H_2O and NO. *Froidevaux and Yung* [1982] have shown that a reduction in the average laboratory values for the O_2 absorption cross section in the 200-230 nm region (Herzberg continuum) results in significant improvement between calculated and observed chlorofluorocarbon vertical profiles [see also *Brasseur et al.*, 1983]. In situ observations of solar fluxes transmitted down to the 30-40 km region [*Frederick and Mentall*, 1982; *Herman and Mentall*, 1982; *Anderson and Hall*, 1983] have led to a determination of the O_2 absorption cross sections in the Herzberg continuum, and the results are indeed lower than laboratory data. We have adopted the values from Herman and Mentall in the 205-250 nm region (similar to data of *Shardanand and Prasad Rao* [1977] beyond 215 nm) for model results described here. Between 196 and 205 nm in the Schumann-Runge band region (spectral intervals 1 through 5 in *Allen and Frederick* [1982]), we have reduced our old effective cross sections by a factor of 0.55, which leads to values consistent with the results of Herman and Mentall.

The solar flux values at the top of the atmosphere come from various sources. The accuracy of measurements made from rockets and, more recently, from satellites has improved to the point that the uncertainty in fluxes is about 10% or less. There is, however, some natural variability in the solar output, mostly below 200 nm, in relation to the 27-day solar rotation period as well as the 11-year solar cycle [*Rottman et al.*, 1982; *Mount et al.*, 1980; *Mount and Rottman*, 1981; *Rottman*, 1981; *Lean et al.*, 1982]. The reference solar flux generally used below 315 nm corresponds to the observations near solar maximum of *Mount and Rottman* [1981], while above that wavelength, the tables of *Hudson et al.* [1982] are used. Our models of the ClO diurnal variation that are compared with the most recent observations of ClO [*Solomon et al.*, 1984] used the solar minimum flux measurements of *Mount and Rottman* [1983].

The mean state of the radiation field is determined by

TABLE 1*b*. Photoreactions

	Reaction	Wavelength Range, nm	Photodissociation Rate Constant*, s^{-1} 40 km	20 km	Cross-section Reference†
(1)	$O_2 + h\nu \rightarrow 2O$	$180 < \lambda < 255$	3.15 (-10)	4.19 (-13)	*Allen et al.* [1981], *Allen and Frederick* [1982]
(2)	$O_2 + h\nu \rightarrow O + O(^1D)$	$\lambda < 175$	<1 (-40)	<1 (-40)	*Allen et al.* [1981], *Allen and Frederick* [1982]
(3)	$O_3 + h\nu \rightarrow O_2 + O$	$200 < \lambda < 800$	7.20 (-4)	5.75 (-4)	*Allen et al.* [1981], *Nicolet* [1978]
(4)	$O_3 + h\nu \rightarrow O_2 + O(^1D)$	$170 < \lambda < 317.5$	1.18 (-3)	2.19 (-5)	*Allen et al.* [1981], *DeMore et al.* [1982]
(5)	$H_2O + h\nu \rightarrow H + OH$	$\lambda < 200$	2.94 (-9)	1.61 (-12)	*Allen et al.* [1981]
(6)	$H_2O_2 + h\nu \rightarrow 2OH$	$\lambda < 352.5$	3.89 (-5)	1.06 (-5)	*DeMore et al.* [1982], *Hudson and Kieffer* [1975]
(7)	$N_2O + h\nu \rightarrow N_2 + O(^1D)$	$\lambda < 240$	3.11 (-7)	9.70 (-10)	
(8)	$NO + h\nu \rightarrow N + O$	$\lambda < 200$	1.94 (-7)	1.07 (-12)	*Allen and Frederick* [1982]
(9)	$NO_2 + h\nu \rightarrow NO + O$	$\lambda < 420$	1.23 (-2)	1.24(-2)	*DeMore et al.* [1982], *Nicolet* [1978]
(10)	$NO_3 + h\nu \rightarrow NO_2 + O$	$470 < \lambda < 630$	2.45 (-1)	2.46 (-1)	*Magnotta and Johnston* [1980]
(11)	$NO_3 + h\nu \rightarrow NO + O_2$	$590 < \lambda < 630$	2.83 (-2)	2.84 (-2)	*Magnotta and Johnston* [1980]
(12)	$N_2O_5 + h\nu \rightarrow 2NO_2 + O$	$205 < \lambda < 382.5$	2.68 (-4)	2.32 (-5)	
(13)	$HNO_3 + h\nu \rightarrow NO_2 + OH$	$190 < \lambda < 327.5$	6.52 (-5)	8.74 (-7)	
(14)	$HO_2NO_2 + h\nu \rightarrow HO_2 + NO_2$	$190 < \lambda < 327.5$	1.56 (-4)	9.80 (-6)	
(15)	$HNO_2 + h\nu \rightarrow OH + NO$	$312.5 < \lambda < 392.5$	2.40 (-3)	2.46 (-3)	
(16)	$CFCl_3 + h\nu \rightarrow 3Cl$ + products	$175 < \lambda < 257.5$	7.10 (-6)	2.38 (-8)	
(17)	$CF_2Cl_2 + h\nu \rightarrow 2Cl$ + products	$175 < \lambda < 240$	6.68 (-7)	1.53 (-9)	
(18)	$CCl_4 + h\nu \rightarrow 4Cl$ + products	$175 < \lambda < 272.5$	1.56 (-5)	3.58 (-8)	
(19)	$C_2H_3Cl_3 + h\nu \rightarrow 3Cl$ + products	$180 < \lambda < 240$	8.99 (-6)	3.02 (-8)	
(20)	$CH_3Cl + h\nu \rightarrow Cl + CH_3$	$175 < \lambda < 220$	1.78 (-7)	5.34 (-10)	
(21)	$C_2F_3Cl_3 + h\nu \rightarrow 3Cl$ + products	$180 < \lambda < 220$	1.18 (-6)	3.73 (-9)	*Nicolet* [1978]
(22)	$C_2F_4Cl_2 + h\nu \rightarrow 2Cl$ + products	$175 < \lambda < 220$	8.27 (-8)	2.53 (-10)	*Nicolet* [1978]
(23)	$ClONO_2 + h\nu \rightarrow Cl + NO_3$	$185 < \lambda < 450$	2.89 (-4)	6.36 (-5)	
(24)	$HOCl + h\nu \rightarrow OH + Cl$	$195 < \lambda < 420$	4.60 (-4)	3.63 (-4)	
(25)	$ClO + h\nu \rightarrow Cl + O$	$200 < \lambda < 337.5$	1.26 (-3)	7.33 (-5)	*Nicolet* [1978], *Langhoff et al.* [1977]
(26)	$HCl + h\nu \rightarrow H + Cl$	$\lambda < 230$	2.56 (-7)	8.06 (-10)	*Inn* [1975], *Myer and Samson* [1970]
(27)	$CO_2 + h\nu \rightarrow CO + O$	$\lambda < 205$	2.49 (-11)	1.93 (-14)	*Allen et al.* [1981]
(28)	$H_2CO + h\nu \rightarrow HCO + H$	$240 < \lambda < 332.5$	6.37 (-5)	3.32 (-5)	
(29)	$H_2CO + h\nu \rightarrow H_2 + CO$	$240 < \lambda < 362.5$	1.02 (-4)	9.31 (-5)	
(30)	$CH_3OOH + h\nu \rightarrow CH_3O + OH$	$205 < \lambda < 352.5$	3.36 (-5)	1.01 (-5)	
(31)	$CH_3O_2NO_2 + h\nu \rightarrow CH_3O_2 + NO_2$	$200 < \lambda < 312.5$	1.88 (-4)	1.67 (-5)	*Baulch et al.* [1982]
(32)	$COF_2 + h\nu \rightarrow 2F + CO$	$185 < \lambda < 225$	1.48 (-7)	5.05 (-10)	

TABLE 1*b*. Photoreactions

	Reaction	Wavelength Range, nm	Photodissociation Rate Constant*, s^{-1} 40 km	20 km	Cross-section Reference†
(33)	$COFCl + h\nu \rightarrow F + Cl + CO$	$185 < \lambda < 225$	3.50 (-6)	6.88 (-9)	
(34)	Extinction by NO_2	$\lambda < 710$			*R.J. Gelinas* [unpublished manuscript, 1974], *DeMore et al.* [1982]
(35)	Rayleigh scattering	$292.5 < \lambda < 800$			see text

* Values listed are for a solar zenith angle of 45°. The U.S. Standard Atmosphere 1976, was used in these calculations, and multiple scattering (with a Lambert albedo of 0.25 for the ground) was included.

† Unless otherwise stated, reference is *DeMore et al.* [1982].

molecular absorption by O_2, O_3, and NO_2, as well as Rayleigh scattering and ground Lambert reflection (albedo equal to 0.25 for our mid-latitude models). Throughout this work, except for subsection 2.2, we combine the direct flux in a spherical shell atmosphere with the diffuse component calculated in a plane parallel geometry. The direct flux is obtained through a geometrical ray-tracing calculation, whereby the slant optical depth is computed along the path. This provides a more accurate evaluation than the Chapman function formulation in the case of absorbers such as ozone, whose concentration peaks in the lower stratosphere [see *Froidevaux*, 1983, for further details]. Multiple scattering has been shown to have a significant effect on photodissociation rates and photochemistry in the stratosphere [*Callis et al.*, 1975; *Sundararaman*, 1975; *Luther and Gelinas*, 1976; *Isaksen et al.*, 1977; *Luther et al.*, 1978; *Pitari and Visconti*, 1979; *Fiocco*, 1980; *Meier et al.*, 1982; *Nicolet et al.*, 1982], mostly for wavelengths longer than 300 nm. We have added the diffuse to the direct flux in our model for λ between 290 and 800 nm. The diffuse intensity is calculated by solving the radiative transfer equation for an inhomogeneous plane parallel atmosphere via the Feautrier method [*Feautrier*, 1964; see also *Prather*, 1974; *Gladstone*, 1982]. We have tested our calculations against those of *Luther and Gelinas* [1976]. We find essentially identical results and we will not duplicate their graphs here (see *Froidevaux* [1983] for some plots of our model photodissociation rates).

Various approaches to diurnally averaged calculations have been presented by *Whitten and Turco* [1974], *Kurzeja* [1975, 1977], *Martin* [1976], *Cogley and Borucki* [1976], *Rundel* [1977)], *Kramer and Widhopf* [1978], *Turco and Whitten* [1978], and *Boughner* [1980]. In our diurnally averaged, steady state computations the mean radiation field for a 24-hour period is derived by calculating the diurnally averaged atmospheric opacity at each altitude and wavelength. The variation of the daylight period with altitude is taken into account. Calculating diurnally averaged chemical reaction rates accurately is difficult, since the rates are the products of diurnally varying concentrations. Fortunately, most of the long-lived species are destroyed by photolysis. For the best comparison with observations the concentrations of the chemically more reactive species are usually derived from diurnal calculations. It is interesting to note that, in the case of O_3, the diurnally averaged results and a 24-hour average of the diurnal values are within 10% of each other. However, the one-dimensional calculations of long-lived species are basically flawed as the result of an inaccurate inclusion of seasonal transport effects, so the results presented here are, at best, representative of an annually averaged mean state of the atmosphere.

2.2. *Diffuse Flux in a Spherical Shell Atmosphere*

In this section we attempt to explicitly demonstrate the effect of sphericity in the atmosphere on the diffuse radiation field and, more importantly, on the concentrations of trace species. *Hudson and Reed* [1979] indicated that the assumption of a plane parallel atmosphere for the diffuse flux was one source of model uncertainty, particularly at large zenith angles. This is an important point because many of the observations with which models are compared have been obtained near sunrise or sunset. In this paper we will be emphasizing a detailed analysis of the ClO diurnal profile. Therefore we proceed to quantify to first order, for solar zenith angles close to 90°, the impact of the plane-parallel atmosphere assumption in calculating the diffuse radiation field and, more importantly, the trace species concentrations in the stratosphere. We are not aware of any previously published discussion of this question.

A first-order approximation to the effects of sphericity can be introduced by modifying the plane parallel slant optical depth (τ/μ_o) to the appropriate value in the single-scattering term of the equation of radiative transfer. Some authors have used this in their photochemical model but without an explicit description of the associated effects. The modification of slant opacity (τ_s) can be made by using the Chapman function, but we have used the geometric ray path approach. We first present results for a homogeneous and conservative atmosphere (τ_s can be evaluated analytically in the homogeneous case) in order to compare them with the diffuse intensities of the backward Monte Carlo calculations of *Adams and Kattawar* [1978]. The results at large solar zenith angle ($\chi = 84.26°$) are shown in Figure 2, for total normal optical depths τ_1 of 0.25 and 1.00, as a

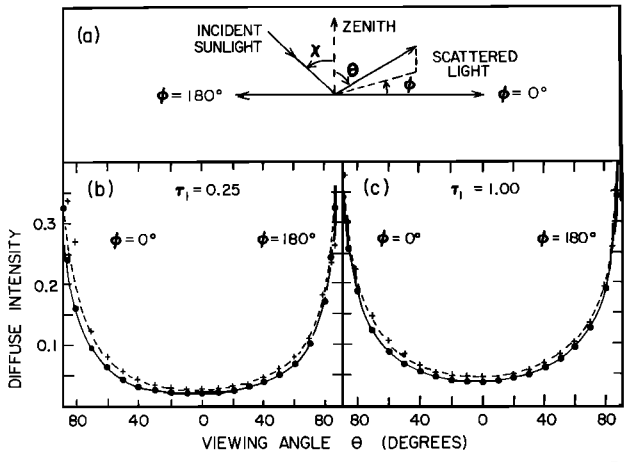

Fig. 2. Model diffuse intensities (normalized to an input solar flux of π) at the top of a 100-km-thick, homogeneous and conservative plane parallel (solid line) or spherical shell (dashed line) atmosphere of total normal optical depth τ_1 (0.25 or 1.00), for a solar zenith angle χ of 84.26°. Results as a function of viewing angle Θ for two values of azimuth angle (Φ = 0° and Φ = 180°) are shown; angles are defined in top part of figure. The Monte Carlo results of *Adams and Kattawar* [1978] are shown (solid circles for plane parallel and crosses for spherical shell) for comparison. Our spherical shell approximation includes the first-order single-scattering correction (see text).

function of viewing angle Θ at the top of the atmosphere and for two azimuthal directions (Φ = 0 and 180°). The plane parallel calculations are in excellent agreement with each other. If sphericity is included, more direct radiation, and therefore a higher single scattered intensity, will be present throughout the atmosphere. The correction to the single-scattering term in the radiative transfer program leads to intensities very similar to the Monte Carlo results for $\Theta \lesssim 75°$. At larger viewing angles the two calculations show some disagreement. However, in terms of photochemical effects the integral of the intensity over solid angle is the relevant quantity, and this diffuse flux is not very sensitive to the intensity changes at large Θ. Recently, *Anderson* [1983] has shown that the use of plane-parallel geometry for multiple scattering and spherical geometry for single scattering leads to relatively small errors in the fluxes as long as the solar zenith angle is less than 95°.

We now quantitatively describe the effects of sphericity on the diffuse fluxes, photodissociation rates, and species concentrations in the earth's stratosphere. Only the first-order correction for single scattering is included. The importance of the diffuse flux relative to the total radiation field depends on the wavelength but increases with solar zenith angle. At wavelengths where strong absorption occurs (short of ~300 nm) the diffuse flux accounts for a large fraction of the total flux, but it is highly attenuated. Molecular photodissociation rate constants will be affected more (in terms of total flux) by the longer wavelengths. In the Chappuis band (400-800 nm) the small total opacity (Rayleigh + ozone) leads to a large direct flux relative to the total flux. Species such as HNO_3 and HO_2NO_2, whose photodissociation occurs short of 330 nm, are most affected by the diffuse flux effect just beyond 300 nm and in the lower stratosphere. The most significant changes in photodissociation rate constants due to the inclusion of sphericity in the diffuse flux calculations are plotted in Figure 3 as percent increases versus altitude for a solar zenith angle of 88.5°. We have included the effect of sphericity on the diffuse fluxes in a diurnal calculation (32°N latitude, -11° solar declination (latitude of subsolar point), COSPAR International Reference Atmosphere (CIRA) 1972 April background atmosphere) in order to investigate changes in species concentrations. The increased rates of photolysis near sunset or sunrise do not affect the "long-lived" (lifetime longer than an hour) species, since they cannot respond very fast. As illustrated in Figure 4 for a height of 20 km, where the diffuse flux plays a large role, the short-lived radicals such as O, OH, *Cl*O, NO, NO_2, and NO_3 display the effect of the above increases in photodissociation rates. The abundance of $O(^1D)$ is also significantly increased (by up to 30% in the lower stratosphere). The ozone photodissociation rate increase leads to more O and $O(^1D)$. Moreover, [H], [OH], and $[HO_2]$ are all affected in a similar fashion by increased $j(HNO_3)$ and $j(HO_2NO_2)$ near 90° in the lower stratosphere. The NO concentration is increased as a result of the larger $j(NO_2)$, $[NO_2]$ itself is decreased somewhat, while $[NO_3]$ decreases because of less $[NO_2]$ and a higher $j(NO_3)$. Chlorine nitrate photolysis leads to an enhancement in the chlorine radicals (*Cl*, *Cl*O, *Cl*OO), although only [*Cl*O] is plotted in the figure. The [OH] radical shows the largest change, close to a 20% increase at the terminator. For most other radicals, less than 10% change occurs for zenith angles below 90°, with the effect diminishing at higher altitudes.

The above study shows that for most species, including short-lived radicals, the model's omission of spherical geometry effects on the diffuse flux will not produce significant or measurable (over 10%) changes in predicted stratospheric concentrations for χ less than 90°. The main exception concerns HO_x (OH and HO_2), for which the predicted lower-stratospheric increase in concentration is close to 20% near 90°. Moreover, this effect increases rapidly as χ increases, and an extrapolation to twilight effects would indicate that the HO_x radical concentrations are underestimated in the standard model by more than 50% for solar zenith angles larger than 92° (in the lower stratosphere). We also note that other effects that are not

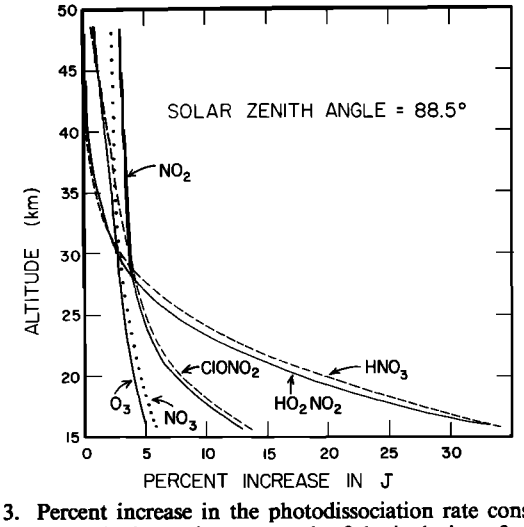

Fig. 3. Percent increase in the photodissociation rate constants of certain stratospheric species as a result of the inclusion of sphericity in the single-scattered intensities, for a solar zenith angle of 88.5°.

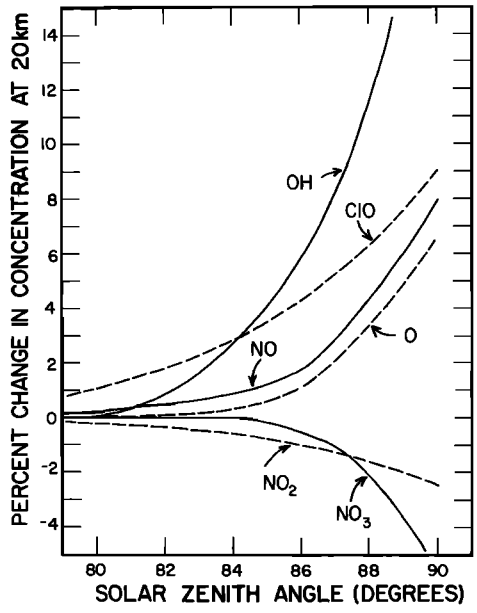

Fig. 4. Effect of changes in the photodissociation rates (as shown in Figure 3 for 88.5° and explained in the text) on short-lived radical concentrations near sunset, at an altitude of 20 km.

included in photochemical models, such as refraction or aerosol absorption and scattering are sources of uncertainty, particularly at large zenith angles [*Adams et al.*, 1974; *Blattner et al.*, 1974]. Such uncertainties preclude an exact determination of the chemical abundances of radicals near sunset and sunrise, especially during the twilight period, but are likely to enhance the effect on radical concentrations discussed in this section. The largest predicted changes in these concentrations occur in the lower stratosphere, where the abundances are generally low and difficult to measure (at least for HO_x and ClO_x). Nevertheless, with instrumental enhancements, some of these radicals might soon be measured by occultation techniques. In this case a detailed comparison with model results should attempt to include a more exact calculation of the diffuse flux.

3. HO_x AND NO_x RADICALS

Differences between observations of the O_3 profile in the upper stratosphere and model calculations can result from errors in the calculated concentrations of the radicals involved in the catalytic destruction of O_3. Therefore we precede our discussion of the model O_3 profiles with a comparison between observations for HO_x and NO_x and our model results for these species. The standard model referred to below for comparison with observations (in an average sense) uses an equinox background atmosphere (CIRA 1972 model, nominally for April 1, 30°N), and the radiation field is calculated for 32°N latitude, -11° solar declination. These conditions of solar illumination apply for the February 20 microwave measurements of ClO by *Waters et al.* [1981]. The mid-latitude background atmospheric values of temperature and pressure (at a given height) can change by a few percent from one month to the next, but changes in the radiation field, which drives a large part of the chemistry, are about 10% or significantly more (depending on altitude and wavelength) for a similar time period. Variations in the background atmosphere are therefore of second order, and we consider the use of a few atmosphere cases (such as summer, winter, spring, and fall) sufficient for our purposes here.

3.1. HO_x

Water vapor is the source of HO_x radicals in the stratosphere. In the upper stratosphere our typical mid-latitude model values for H_2O are between 6 and 7 ppmv. The calculated increase above the tropopause (where we have 3.6 ppmv) is due to methane oxidation. These water abundances are similar to the average of a large number of past observations (J. Frederick, private communication, 1983).

Changes in the recommended values of certain laboratory rate constants (in particular for the OH + HNO_3 and OH + HO_2NO_2 reactions) during the last few years have drastically changed the predicted vertical distribution of HO_x radicals in the stratosphere. The effects of such changes on HO_x and other species (such as ClO) have been clearly presented in *Hudson et al.* [1982] and partially discussed in *Sze and Ko* [1981] as well. A considerable reduction occurred in the predicted importance of the HO_x catalytic cycles in the ozone destruction process. More recent studies of the O + HO_2 reaction converting HO_2 to OH [*Keyser*, 1982; *Sridharan et al.*, 1982; *Brune et al.*, 1983] and its associated temperature dependence have increased the recommended rate constant by about 60% at upper stratospheric tempera-

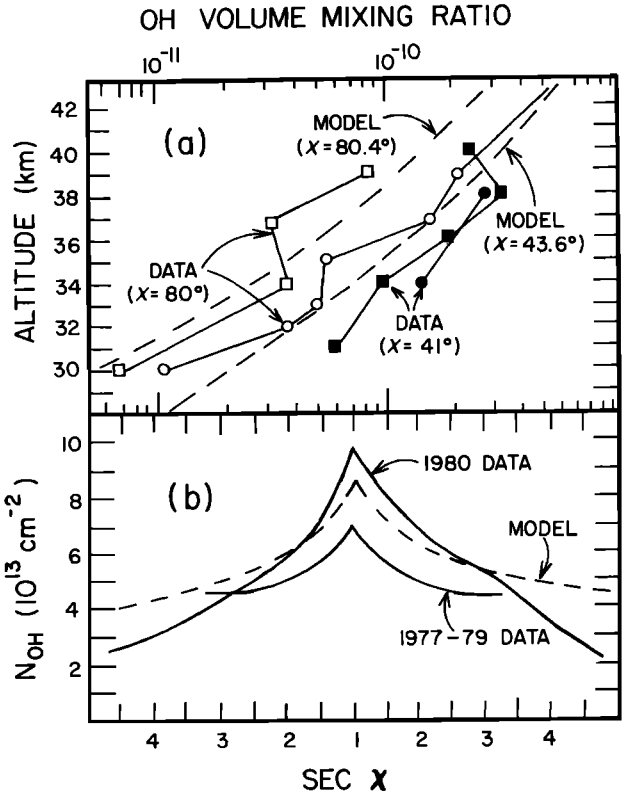

Fig. 5. (*a*) OH volume mixing ratio versus altitude. Data are from resonance fluorescence measurements at 32°N latitude [*Anderson*, 1980]: solid circles (September 20, 1977) and squares (July 14, 1977) are for a solar zenith angle χ of 41°, whereas open circles (January 12, 1976) and squares (April 26, 1977) are for χ = 80°. Results of our standard model are shown for similar values of χ (43.6° and 80.4°) (dashed lines). (*b*) Total OH column abundance above ground level as a function of sec χ. Data from *Burnett and Burnett* [1981, 1982] are shown for 1977-1979 and 1980 averages (solid lines) along with our standard model predictions (dashed line).

tures; this has increased the $[OH]/[HO_2]$ ratio in the upper stratosphere, and [OH] has increased by about 30% near 40 km.

Balloon-borne molecular resonance fluorescence measurements of OH above 30 km at 32° [*Anderson*, 1980] are shown in Figure 5*a*. The averages of the observed profiles for $\chi = 80°$ and $\chi = 41°$ are in good agreement with model results at similar zenith angles, given the observational uncertainties of about ±30%. Ground-based Pepsios spectrometer measurements [*Burnett and Burnett*, 1981, 1982] of OH absorption near 308 nm are plotted versus sec χ in Figure 5*b*. The measured column abundances (N_{OH}) represent fits through average data taken during 1977-1979 and also during solar maximum in 1980; the 1981 data (not shown here) are 3% lower than during 1980, on the average. Our model results (solar maximum flux conditions), extrapolated above 60 km by adding 20% to get the total column amount, agree with both data sets to within 20% for sec $\chi \lesssim 3.5$ ($\chi \lesssim 73°$). The average daytime model OH column abundance is within 15% of the (similarly averaged) Pepsios results, and an extrapolation of Anderson's in situ data agrees with the latter results as well [see *Hudson et al.*, 1982]. The sharp decrease in the observed N_{OH} at large zenith angles is somewhat puzzling if it is real and not caused by some contamination of the absorption feature. A factor of 2 difference near 80° could imply a possible overestimate of $[O(^1D)]$ in the model by a factor of 4 in the upper stratosphere and mesosphere. At noon the model OH column above 45 km provides about half of the total column abundance, and its contribution increases to about two thirds of the total for $\chi \simeq 80°$. The discrepancy at large χ thus seems to imply that a large part of the difference in column amount has to come from the uppermost stratosphere and mesosphere. One expects more sensitivity to $O(^1D)$ and the short-wavelength solar flux producing this radical at the higher altitudes. The discrepancy between observed and calculated ozone abundances in the upper stratosphere (see section 5) could be partly responsible for the high OH column amounts predicted by our model at large solar zenith angles, since a low model ozone column leads to high UV fluxes in the middle stratosphere as well as high $O(^1D)$ and OH concentrations. The limited resonance fluorescence data [*Anderson*, 1980] shown in the figure for $\chi = 80°$ do not show a factor of 2 discrepancy with the model results. However, these data were taken during 1976-1977, and it would be interesting to compare them to later in situ data in order to confirm or deny the temporal variations observed from the ground. There are certain aspects of the ground-based observations that are not clearly understood, such as large sudden changes during the day and larger-than-expected variations as a function of season and solar cycle. Other observations of OH near 35 km by balloon-borne laser radar (lidar) through the afternoon and early evening [*Heaps and McGee*, 1983] show large disagreement with models and other measurements discussed above; in view of this and the large uncertainties associated with these observations we feel that further lidar data are needed for a more accurate test of this method and its repeatability.

The HO_2 radical has been detected a few times in the stratosphere. Several vertical profiles of HO_2 are shown in Figure 6, taken from the recent paper by *de Zafra et al.*

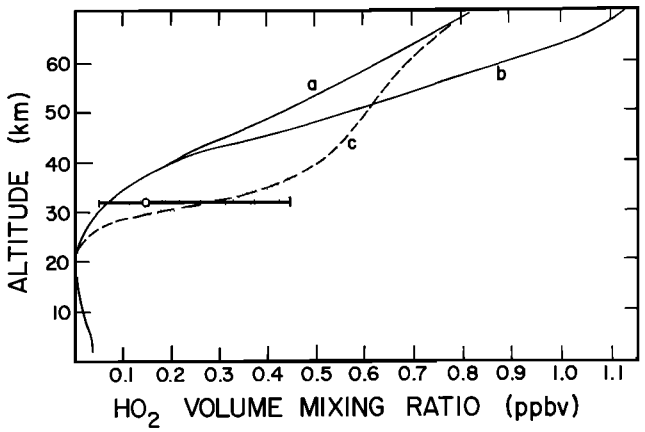

Fig. 6. HO_2 data and theoretical profiles taken from *deZafra et al.* [1984]. Open circle with large error bar is measurement at 53°N by *Mihelcic et al.* [1978] adjusted to midday value, and shaded area represents range of data obtained at 32°N in 1977 by *Anderson et al.* [1981]. Profiles *a* and *b* use somewhat different chemistry (see text), and curve *c* (dashed line) is a rough fit through the Anderson data, extrapolated to model *a* values at 70 km.

[1984]. These authors detected HO_2 from the ground (Mauna Kea, Hawaii, 20°N latitude), during 4 days in September-October 1982, by observing the HO_2 microwave emission lines near 266 GHz. They compared the observed line shape and strength to the line profiles predicted from theoretical HO_2 vertical distributions *a*, *b*, and *c*, shown in the figure. The in situ cold trap measurement by *Mihelcic et al.* [1978] at 32 km is shown in Figure 6, but its associated uncertainty is large. The somewhat indirect in situ observations of HO_2 (conversion via NO to OH followed by resonance fluorescence detection of OH) by *Anderson et al.* [1981] are also illustrated (range of three 1977 measurements). Both of these data sets were taken below the altitude region of most interest to us, in terms of the effect on upper-stratospheric ozone. The main difference from model *b* to model *a* in Figure 6 is an increase in k_{18} ($O + HO_2 \rightarrow OH + O_2$) (as discussed previously), which shifts the value of the ratio $[OH]/[HO_2]$ ($\simeq k_{18} / k_{17}$ above 40 km) and decreases $[HO_2]$. Curve *c* is a rough fit through Anderson's [1982] data combined with a smooth increase toward model profile *a*. The average of 4 days of HO_2 measurements taken between 10 A.M. and 5 P.M. by de Zafra et al. agrees quite well with a synthetic line profile generated from model *a*. As shown by the above authors, model *b* leads to a higher peak line intensity than observed, whereas model *c* provides too much low altitude HO_2 (pressure broadened in the wings of the emission line). Our model results for 20°N latitude, averaged between the appropriate times of observation, are essentially identical to model *a*, as expected, since we are also using laboratory kinetic data taken mostly from *DeMore et al.* [1982]. It is encouraging that the most recent photochemical data (particularly the value for k_{18}) provide the best fit (see model *a* in Figure 6) to the ground-based microwave data. However, we caution that this good agreement might be partly coincidental, since natural variations in H_2O could conceivably lead to HO_2 profiles as different as cases *a* and *b*, and there were no simultaneous measurements of H_2O during the above HO_2 observations. These results show a systematic difference between

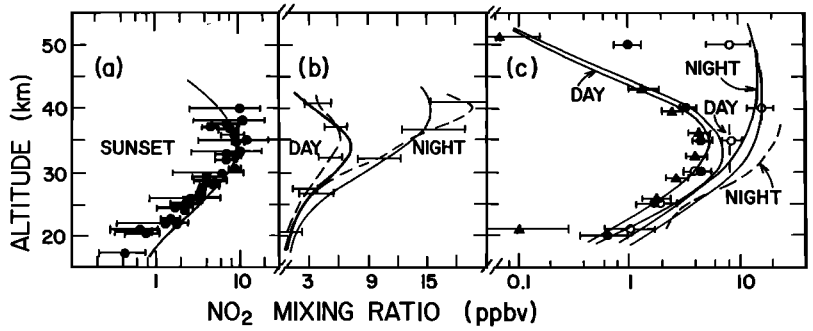

Fig. 7. Comparison of our standard model (32°N latitude, CIRA 1972, April background atmosphere) with various NO_2 observations at mid-latitudes: (*a*) sunset observations taken from summary in *Hudson et al.* [1982]; data were obtained by several different groups (see reference above); model results (solid line) are for $\chi = 90.6°$; (*b*) LIMS day and night data (dashed lines) are compared to model NO_2 profiles for similar times (about 1 and 10 P.M.). Data were taken at 32°N on May 5, 1979 [see *Russell et al.*, 1984]; (*c*) Day-to-night variations in NO_2, as observed by different groups: *Harries* [1978], dashed lines labeled for day and night; *Drummond and Jarnot* [1978], solid circles (day) and open circles (night); *Roscoe et al.* [1981], triangles (day). The two sets of solid lines for the day and night model profiles indicate the predicted variation in the NO_2 abundance for 8-hour periods centered around noon and midnight.

Anderson's in situ data and models that agree with the microwave ground-based data (case *c* versus *a*), although the microwave data are not very sensitive to the abundance of HO_2 below 35 km. We note that most (~80%) of the HO_2 column amount resides below about 50 km for profile *a*, with 40% in the 35-50 km region, where HO_x radicals affect the upper stratospheric ozone abundance. Further observations such as these microwave ground-based measurements therefore have the potential of developing an increasingly accurate picture of the average HO_2 abundance in the upper stratosphere (and mesosphere) along with its seasonal and latitudinal variations. Added benefit for comparison with models would, of course, be provided if H_2O (and OH) data could be obtained concurrently with such HO_2 measurements.

H_2O_2 is closely tied to HO_2 through the $HO_2 + HO_2$ formation reaction and is destroyed by photolysis and reaction with OH. Its chemical lifetime in the stratosphere is long enough that only small diurnal variations in $[H_2O_2]$ are expected. Measurements of $[H_2O_2]$ could provide a sensitive monitor of relative variations in $[HO_2]$ (from day to day or season to season) because of the essentially quadratic type of dependence between these two species. To date, however, only a tentative microwave detection of H_2O_2 has been made because of the low signal-to-noise ratio and possible contamination of the line by other features [*Waters et al.*, 1981]. This detection of about 1.5 ppbv at 30 km is an order of magnitude higher than our model prediction with the temperature-dependent value of k_{26} [*Kircher and Sander*, 1984]. Improved signal to noise in the microwave measurements (cooled radiometer and longer integration times) should be possible in the near future (J. Waters, private communication, 1983), allowing a more definite detection of the stratospheric H_2O_2 abundance. Recently, *Chance and Traub* [1984] have determined an upper limit for H_2O_2 in the 20-40 km region, using far-infrared emission spectra collected from a balloon platform. Their results are in much better agreement with model predictions.

3.2. NO_x

The NO_x radicals (NO and NO_2) are predicted to play an important role in the catalytic destruction of ozone. An overview of NO_x observations shows that, on the average, mid-latitude measurements are in agreement with our standard model, given the uncertainties and variability in some of the data, as discussed below.

Figure 7 summarizes our comparison for NO_2. A large number of observations of NO_2 have been taken during sunset by infrared absorption spectroscopy, as shown in Figure 7*a*. These data are composed of various experiments at different seasons, and the references can be found in *Hudson et al.* [1982]. The average vertical distribution is similar to our standard model sunset results ($\chi = 90.6°$ solid line), although the model profile is somewhat on the high side below about 30 km. In Figure 7*b*, a typical day-to-night variation in NO_2 abundance at 32°N, as measured by the LIMS (Limb Infrared Monitor of the Stratosphere) radiometer [*Russell et al.*, 1984], is compared to our model results for the appropriate latitude and times. The large diurnal variation, theoretically caused primarily by interconversion between NO and NO_2, is evident in both model and observations, which exhibit a similar trend versus height. Earlier observations relating to the diurnal variation of NO_2 in the stratosphere are also shown in Figure 7*c*, following the summary by *Roscoe et al.* [1981]. Our standard model results for day and night (two sets of solid lines) show the predicted range during the 8-hour time periods centered around noon and midnight, respectively. Only a few observations exist for the altitude range above 35 km. Daytime balloon-borne pressure modulated radiometer observations of NO_2 emission at 6.2μm were obtained by *Drummond and Jarnot* [1978] and Roscoe et al. The latter data represent an average daytime result similar to our average model profile. We note that these authors simultaneously obtained NO data that are in fair agreement with our NO model profile from about 35 to 50 km (but drop off much faster below 30 km). The "day" measurements of Drummond and Jarnot were made about 1 hour after sunrise, at a time when the NO_2 abundance starts dropping fairly fast. Nevertheless the corresponding point near 50 km is still significantly higher than expected, although we note that measurements above the balloon float altitude represent average column results and might be more uncertain than indicated.

One should also note the effect of a decreased model OH

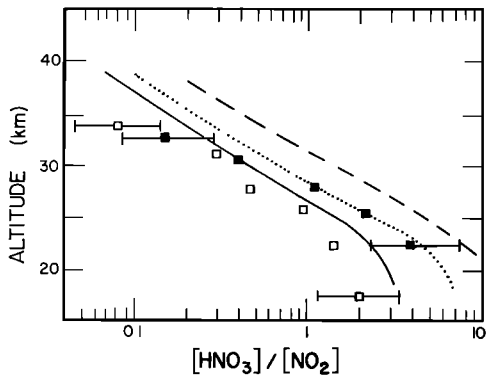

Fig. 8. Predicted values of $[HNO_3]/[NO_2]$ for our standard model (solid line for sunset, dotted line for noon). This is compared to an earlier chemical model (dashed line) and available data taken from *Harries* [1978]. Open squares are sunset data and solid squares are noon data.

abundance in the stratosphere on the ratio of $[HNO_3]$ to $[NO_2]$, written (for daytime) as

$$\frac{[HNO_3]}{[NO_2]} = \frac{k_{45}[M][OH]}{j_{13} + k_{46}[OH]} \quad (2)$$

Even though the above equilibrium relation will not be established instantaneously throughout the day, less [OH] will cause j_{13} to be the dominant term in the denominator, and the above ratio will be nearly proportional to [OH]. Simultaneous observations of NO_2 and HNO_3 led to a significant discrepancy between observed and theoretical values for $[HNO_3]/[NO_2]$, given the chemistry accepted prior to a few years ago [see *Evans et al.*, 1976; *Harries*, 1978]. As surmised by *Evans et al.* [1982], a decrease in [OH] can considerably improve the model fit for the above ratio. In this respect we compare in Figure 8 our standard mid-latitude predictions for the value of $[HNO_3]/[NO_2]$ versus height with observations taken from *Harries* [1978]. The old chemistry model reported by the above author is seen to predict a much larger ratio than our standard model with updated chemistry. We show two curves, for noon and sunset, and the agreement between models and observations is now reasonable and clearly improved with the current chemistry and reduced OH concentrations. More accurate observations should help determine whether this ratio is still a source of some discrepancy in stratospheric chemistry. There are few measurements of HNO_3 above 35 km; some promising results at these higher altitudes have recently been obtained by *Arnold and Qiu* [1984], who used ion mass spectrometer measurements.

We conclude with a summary of various daytime NO mid-latitude data [from *Hudson et al.*, 1982], shown in Figure 9 along with our standard model for the noon NO profile. The range of data is quite large (factor of 2-5). Besides possible errors in measurements and differences between techniques, seasonal variability and transport effects on the long-lived NO_x ($NO + NO_2$) abundance are probably a source of such variations in the NO data. Relatively large seasonal changes in upper stratospheric NO abundance are indeed observed by *Horvath et al.* [1983]. On the average, however, and particularly in the upper stratosphere, our one-dimensional model is not in strong disagreement with the average of existing mid-latitude measurements of the key radicals NO and NO_2.

4. Observations of ClO and its Diurnal Variation

Chlorine radicals (*Cl* and *ClO*) are also predicted to have a large impact on ozone in the upper stratosphere. The partitioning between *ClO* and the reservoir species *HCl* needs to be investigated, but unfortunately, we are still limited to a separate comparison of *ClO* and *HCl* observations (see sub-section 4.1), since no simultaneous measurements of these two species exist. The diurnal variation of *ClO* is examined in detail in sub-section 4.2, in light of recent observations of diurnal changes in *ClO*.

4.1. *Midday ClO*

The vertical distribution of ClO_x reflects a balance between (in large part) the photolysis of halogenated hydrocarbons and the formation of *HCl* through reactions of *Cl* with CH_4, H_2CO, HO_2, and H_2. The latter species will be affected by transport directly (CH_4, H_2) or indirectly (H_2CO comes from CH_4 oxidation and HO_2 from H_2O); see also *Solomon and Garcia* [1984]. The equilibrium relation between *Cl* and *ClO* can be written as

$$\frac{[ClO]}{[Cl]} = \frac{k_{54}[O_3]}{k_{55}[O] + k_{56}[NO]} \quad (3)$$

and is established on the time scale of a few minutes or less in the stratosphere. Since the exchange between *Cl* and *HCl* takes place on a time scale of order 1 day (upper stratosphere) to 1 month (lower stratosphere), an equilibrium relationship between these two species may hold in a temporally averaged sense. Diurnal changes in ClO_x are

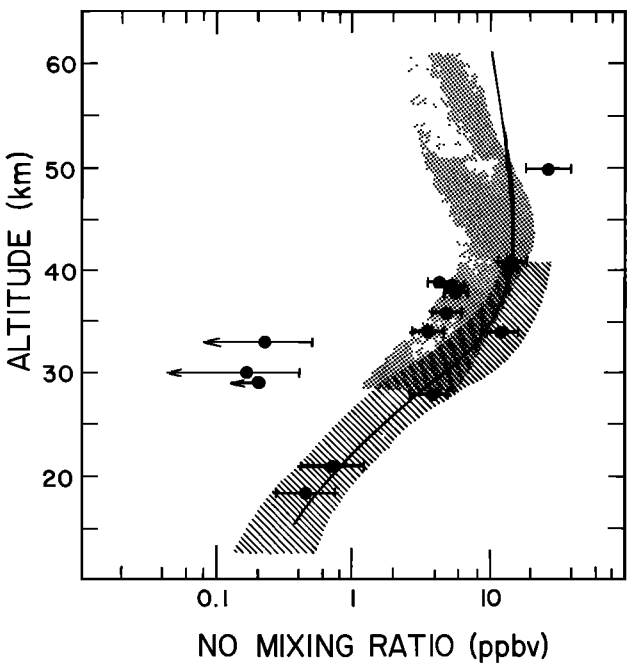

Fig. 9. Summary of mid-latitude daytime NO observations (from *Hudson et al.* [1982], where data references can be found) compared to our standard model results for noon (solid line). Data include in situ and remote observations.

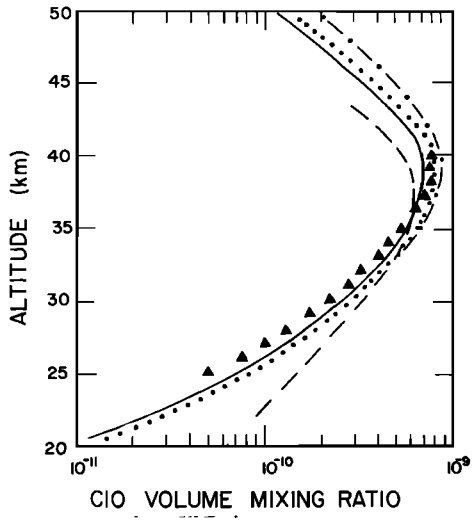

Fig. 10. ClO model profiles compared to the mean of the daytime resonance fluorescence measurements (solid triangles), excluding the anomalously high July 14, 1977, data [see *Anderson et al.*, 1980; *Weinstock et al.*, 1981]. Earlier chemistry is illustrated by model of *Logan et al.* [1978], see dashed line, and compared to our standard model (solid line) for similar solar zenith angles (37° and 44°, respectively). Effects of an increase in k_{60} (OH + HCl reaction) and an additional decrease in k_{55} (O + ClO reaction), as discussed in text, are illustrated by the dotted and dash-dotted lines, respectively.

presumably due to exchange processes with a shorter-lived species (namely $ClONO_2$). With this in mind, we write

$$\frac{[Cl]}{[HCl]} = \frac{k_{60}[OH]}{k_{61}[CH_4] + k_{62}[HO_2] + k_{63}[H_2] + k_{64}[H_2CO] + k_{65}[H_2O_2]} \quad (4)$$

and the ratio [ClO]/[HCl] is then obtained from the product of equations (3) and (4). For the lower stratosphere, where $k_{55}[O] << k_{56}[NO]$ and $k_{61}[CH_4]$ is the dominant term in the denominator of (4), we obtain the familiar expression

$$\frac{[ClO]}{[HCl]} = \frac{k_{54}k_{60}[O_3]}{k_{56}k_{61}[CH_4]} \frac{[OH]}{[NO]} \quad (5)$$

This is one example of the interdependence between HO_x, NO_x, and ClO_x species. Our previous comment about transport also applies in terms of the ClO dependence on OH and NO abundances, which are sensitive to the long-lived source species H_2O and N_2O (or total NO_y). An ideal experimental test of the above relationship would require a simultaneous measurement of all six gases involved, as well as temperature. Such measurements are difficult and not yet available, so that models are best compared with an average of the observational data currently available.

A large number of daytime ClO measurements has been acquired from in situ resonance fluorescence balloon observations [*Anderson et al.*, 1980]. The observations cover the period 1976-1979, and the mean of these data, excluding the anomalously high July 14, 1977, profile was compared in *Weinstock et al.* [1981] to a model by *Logan et al.* [1978]. The spread in the nine observational ClO profiles is quite large (factor of 2-3 from the mean), although the gradient versus height is fairly well represented by the mean profile. As illustrated in Figure 10, earlier models (such as *Logan et al.* [1978]) did not give a satisfactory fit to the observed average ClO profile shape. The later increases in laboratory rate constants for OH + HNO_3 and OH + HO_2NO_2 significantly improved the lower stratospheric ClO model fits because of the resulting reduction in the OH concentration. Further changes in the kinetics since the WMO report [*Hudson et al.*, 1982] would also tend to improve the upper stratospheric ClO model profile. The increase in the adopted value of k_{18} (O + HO_2 reaction), as discussed in the HO_x section above, has led to an increase in model OH concentrations in the upper stratosphere (where atomic oxygen becomes more abundant). This, coupled with a small decrease in predicted CH_4 (because of more OH), leads to a 40% increase in ClO_x near 40 km, since exchange between ClO_x and HCl is mainly governed by the Cl + CH_4 and OH + HCl reactions [see also *Ko and Sze*, 1983]. The overall shape and magnitude of the ClO profile has therefore been favorably modified by a combination of changes in the kinetics, as illustrated by our standard model profile (solid line) in Figure 10.

Two additional changes in laboratory data have been suggested more recently, both of which also tend to increase the upper stratospheric ClO mixing ratio, as shown in Figure 10. *Molina et al.* [1984] find a value for k_{60} (OH + HCl reaction) of $4.6 \times 10^{-12} \exp(-500/T)$ cm^3 s^{-1}. The temperature dependence is not much different from our standard expression for k_{60}, but the difference in A factor leads to a 20% increase (nearly independent of T) in this rate constant. The resulting increase in ClO ranges from 10% near 30 km to over 20% at 50 km (dotted line versus solid line in Figure 10). The associated decrease in HCl is everywhere less than 10%. A recent kinetic study by *Keyser* [1984] agrees (within ±10%) with the above laboratory data on the OH + HCl reaction and points to a higher rate constant than previously recommended. However, since several previous studies of k_{60} were in excellent ($\lesssim$10%) agreement and the differences that now exist are not well understood, it is not clear that one should adopt a higher value for this rate constant. The recent measurement of k_{55} (O + ClO → Cl + O_2) by *Leu* [1984] yields $4.8 \times 10^{-11} \exp(-96/T)$ cm^3 s^{-1}. Our adopted (standard) value is about 40% higher, independent of temperature. Recent laboratory work on the O + ClO reaction by a number of workers would seem to confirm a reduction in k_{55}. Compared to the room temperature (298 K) value of 3.6×10^{-11} cm^3 s^{-1} found by *Leu* and the earlier recommendation of *DeMore et al.* [1982] of 5.0×10^{-11} cm^3 s^{-1}, values of 4.2 ± 0.8, 3.6 ± 0.5, and 3.5 ± 0.5 × 10^{-11} cm^3 s^{-1}) have been obtained by *Margitan* [1984], *Ongstad and Birks* [1984], and *Schwab et al.* [1984], respectively. If one considers systematic errors rather than experimental precision (repeatability) alone, the total uncertainty in all the above determinations is most likely close to ±20% (J. Margitan, private communication, 1984). The temperature dependence of k_{55} is clearly small but will also contribute to the uncertainty (by maybe 15%). Indeed, for most reactions, some of which have been studied more extensively than the

O + ClO reaction (and some of which are easier to study), there seems to exist an error limit of 10%-15% above which the uncertainties in rate constants and the differences between various groups (with sometimes similar techniques) lie. Whatever its exact value, a decrease in k_{55} will decrease the [Cl]/[ClO] ratio above 35 km, where the O + ClO reaction becomes important in the conversion of ClO to Cl. As shown in Figure 10 (dash-dotted line versus dotted line) the incremental increase in [ClO] for k_{55}, according to *Leu*, is about 10% near 40 km and increases to 35% at the stratopause; both diurnal average and diurnal sensitivity tests yield similar results. Since the O + ClO reaction is the rate-limiting step in the major chlorine catalytic cycle destroying ozone, we also expect changes in $[O_3]$ from a decrease in k_{55}. Small changes in our model abundances of present-day ozone occur with a peak increase close to 5% at 40 km.

The daytime (between noon and 4 P.M. local time) balloon-borne microwave observations of ClO by *Waters et al.* [1981] are compared to our standard model for 2:00 P.M. in Figure 11. Good agreement for both the ClO and simultaneously measured O_3 profiles is found, although the slope of the ClO profile between 30 and 23 km seems somewhat steeper than in the model (note the large uncertainty in the observation at 23 km). Other measurements of ClO in the stratosphere via ground-based microwave spectral observations [*Parrish et al.*, 1981] are consistent with the above data. New ground-based microwave observations [*Solomon et al.*, 1984] have been performed in Hawaii and show a strong diurnal behavior, as discussed in the next section. The midday ClO column densities deduced by the microwave ground-based observations have values of 0.9×10^{13} cm^{-2} [from *Parrish et al.*, 1981], 0.7×10^{13} cm^{-2}, and 0.8×10^{13} cm^{-2} [from *Solomon et al.*, 1984], on average about 25% less than the mean of J. Anderson's data presented in Figure 11. Given the large spread in the in situ data, this should be viewed as a good (if not coincidental) agreement. The reevaluated laser heterodyne radiometer measurements of ClO at sunset by *Menzies* [1983] and the attempted ground-based infrared measurements by *Mumma et al.* [1983] are discussed later since they pertain more directly to the diurnal changes in the ClO profile.

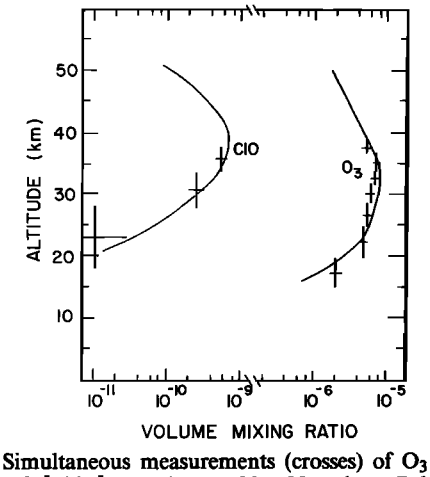

Fig. 11. Simultaneous measurements (crosses) of O_3 and ClO by *Waters et al.* [1981] on February 20, 1981, above Palestine, Texas. Our standard model profiles (solid lines) for similar conditions of illumination (2 P.M. local time) are shown for comparison.

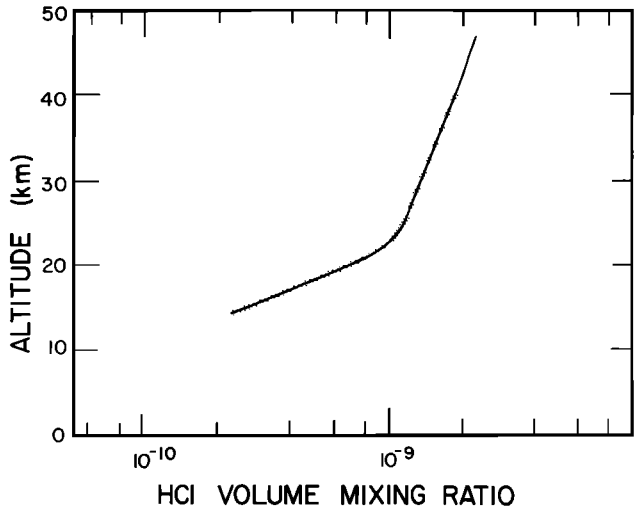

Fig. 12. Range of mid-latitude HCl infrared absorption data [see *Hudson et al.*, 1982] is illustrated by shaded area, and solid line is our standard HCl model profile.

The chlorine reservoir, HCl, has been measured mostly by near-infrared ground-based and balloon-borne absorption spectroscopy. As shown in the summary report by *Hudson et al.* [1982], model profiles fall within the bounds of these observations and roughly follow the observed vertical mean profile. A similar result is illustrated in Figure 12 for our standard model conditions. Reasonable changes in $K(z)$ and seasonal changes (in solar radiation) can modify this one-dimensional profile by about 30%. Lower-stratospheric [HCl] seems somewhat high in most models, particularly at higher latitudes (e.g., 2-D model of *Miller et al.*, [1981]). Aerosols might be contributing to a chlorine sink below ~25 km, although quantitative information on this subject is lacking. The slope of our HCl profile is somewhat different from the mean data and most individual observations (see also summary of data in *Zander* [1981], or *National Research Council* [1982]). However, significant differences exist between the observations themselves, presumably related to the combined effects of transport and chemistry. The upper stratospheric HCl mixing ratio (near 50 km) is close to the total chlorine amount available in the stratosphere and should be increasing slowly with time because of anthropogenic sources. This upper stratospheric value is close to 2.6 ppbv in our mid-latitude models. However, it is worth noting that we have fixed the ground level values for the halocarbons in the steady state model. This leads to a constant total Cl_x value in the upper stratosphere and mesosphere, which is not strictly realistic. Indeed, *Gidel et al.* [1983] use a time-varying upward flux of halocarbons at the ground and obtain a decrease in total Cl_x of about 30%-40% between the ground and 40 km for the year 1980. Therefore, although our tropopause values for total Cl_x agree well with the above author's results, our upper stratospheric values are higher than theirs by about 20%.

4.2. *Diurnal Variation of ClO*

The previous section described measurements and models of the midday ClO profile and the diurnally invariant HCl profile. The other major active chlorine compound is chlorine nitrate ($ClONO_2$), which builds up at night through

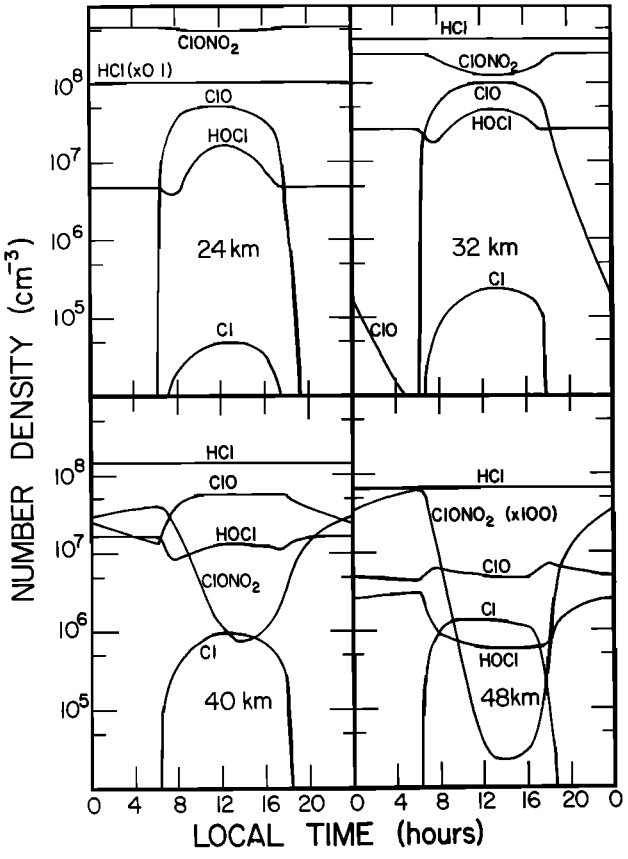

Fig. 13. Calculated diurnal variation of active chlorine species at 24, 32, 40, and 48 km for 32°N latitude, -11° solar declination, and CIRA 1972 April background atmosphere. Long-lived species concentrations are fixed at values obtained from diurnal average model.

the recombination reaction $ClO + NO_2 + M$ and photodissociates during the day to regenerate the chlorine radicals. Its abundance peaks in the lower stratosphere and decreases sharply in the upper stratosphere as a result of the decrease in $[NO_2]$ and [M]. HOCl is a reservoir of secondary importance (according to current photochemistry) formed from the radicals ClO and HO_2 and destroyed mainly by photolysis. The resulting diurnal variation of the active chlorine species is illustrated for various altitudes in Figure 13 (standard model as before). Observations of the ClO diurnal variation in the stratosphere can provide indirect evidence for the main "breathing cycle" between ClO and $ClONO_2$, even though chlorine nitrate is not measured directly. A possible $ClONO_2$ detection (by infrared absorption) near 30 km has been reported by *Murcray et al.* [1979], although this is a difficult measurement and, at best, represents an upper limit consistent with model values [*Hudson et al.*, 1982]. To first order, the sum $[ClO] + [ClONO_2]$ will be constant during the diurnal cycle, and the combined abundance depends on the partitioning with HCl. The effect of chlorine nitrate is to reduce the amount of free radicals (Cl and ClO) available to destroy ozone, although the largest $ClONO_2$ abundance occurs below the altitude (~40 km) of peak efficiency in the chlorine catalytic cycle. We note that we have used a rate of $ClONO_2$ formation in accord with the "fast" value for k_{64} recommended in *DeMore et al.* [1982] and consistent with the absence of other isomers, as implied by recent laboratory work [*Margitan*, 1983; *Cox et al.*, 1984].

Several existing ClO observational data sets reflect the diurnal variation of ClO and the possible interchange with chlorine nitrate. The balloon-borne laser heterodyne radiometer measurements by *Menzies* [1979] showed a measurable ClO absorption feature in the vibration-rotation band near 12 μm. The resulting profiles were significantly higher than model predictions, but new laboratory spectroscopic data have revealed that the ClO observations were referring to an incorrect line position. A reevaluation of the observations [*Menzies*, 1983] in terms of another spectral line apparently due to ClO has led to a sunset ($\chi = 94°$) upper stratospheric profile, as shown in Figure 14. These November 1979 data are compared with our standard mid-latitude diurnal model plotted for solar zenith angles from noon to sunset. The observation at 36 km is an upper limit, which is not as satisfying as a definite detection, but agrees with the steep gradient versus height obtained at higher altitudes. This slope, rather than the absolute amount of ClO, constitutes the main difference between these results and model profiles. Other comparisons regarding the diurnal variation of ClO are now presented, prior to a discussion of model uncertainties that might be a source of the above discrepancy.

Balloon-borne observations of part of the ClO diurnal cycle have been performed by *Waters et al.* [1981]. These are microwave limb sounding measurements of the thermal emission from a ClO rotational transition near 204 GHz. The antenna beamwidth of 0.3° is mostly sensitive to an emission region about 4 km wide at the tangent altitude. The pointing uncertainty is believed to be ± 1 km. The data shown in Figure 15 are proportional to the ClO column abundances between about 28 and 34 km (and to the integrated antenna temperatures) as a function of local time. The measurements for February 20, 1981 [*Waters et al.*, 1981] and May 12, 1981 (unpublished observations by the same group) were obtained above Palestine, Texas and are compared with model results for similar conditions (solar declination of -11° and +18°, respectively) at 32°N latitude. The scaling of the model for noon is somewhat

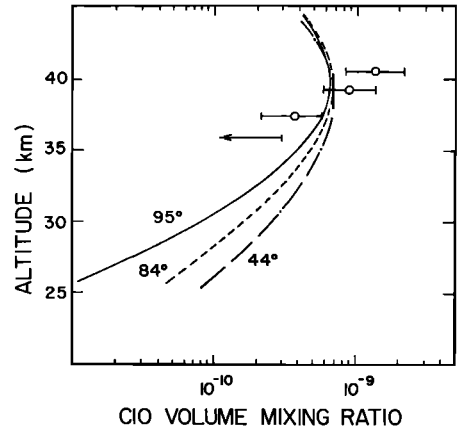

Fig. 14. Reevaluated November 1979 ClO data [*Menzies*, 1983] obtained at sunset by laser heterodyne radiometer measurements (open circles). Model ClO profiles are shown for various solar zenith angles. The curve for 95° corresponds to the time of observations.

arbitrary and the two separate curves shown for each flight were obtained by integrating over ± 3 km around 29 and 31 km, respectively, to (conservatively) account for the pointing uncertainty as well as the antenna beamwidth. Absolute concentrations near 2 P.M. for the February flight compared favorably with our model, as shown previously in Figure 11. The observed relative decrease from noon to sunset also agrees with our model results, given the apparent scatter and uncertainties in the data points. The May observations from sunrise to noon show a slower increase than model predictions, even if one were to choose a noon value less than half of the noon February value.

More recently, ground-based microwave measurements of ClO have been obtained [*Solomon et al.*, 1984] at Mauna Kea, Hawaii (20°N latitude), during October 1-15, 1982, and December 9-16, 1982. The ClO rotational emission line at 278 GHz was observed fairly continuously during these periods, both at day and at night. The data are averaged over several days of observation to obtain a signal-to-noise ratio of about 20 to 1. The column amounts deduced from the microwave ground-based measurements are mostly sensitive to the ClO abundance above 30-32 km, which corresponds to a region within ±50 MHz from the line center; this is due to the pressure-broadening effect in the wing of the line. We have used two models for 20°N latitude and -4° (October) or -23° (December) solar declination for comparison. In Figure 16 (kindly provided by P. Solomon) the emitted line intensity (in millidegrees K) as a function of frequency (or channel number) is shown for the December data. Average daytime (1200-1600 hours) and nighttime (0000-0600 hours) results (for both model and observations) are presented in parts *a* and *b* of the figure, respectively. The synthetic line profiles generated with our model results have been scaled down by a factor of 0.85. The agreement with the observed daytime line shape is very good. At night an additional scaling factor of about 0.8 would be needed for a best fit.

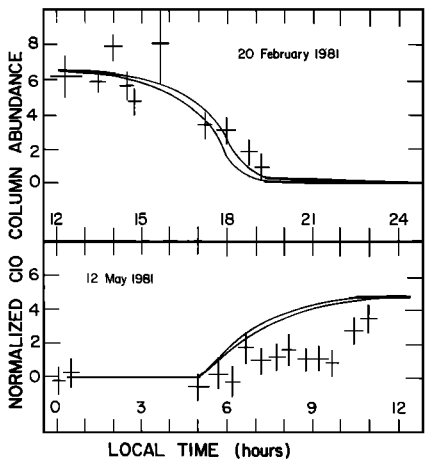

Fig. 15. Comparison of balloon-borne microwave observations of ClO diurnal variation [*Waters et al.*, 1981, and unpublished data of J. Waters, for May 1981] with model results. Crosses indicate average data for each time period, with associated uncertainties. These data are proportional to the ClO column abundances between about 28 and 34 km (and to the integrated antenna temperatures). The two model curves for each flight correspond to the diurnal variation of the ClO abundance integrated over ±3 km around 29 and 31 km, scaled to the adopted noon value (see text).

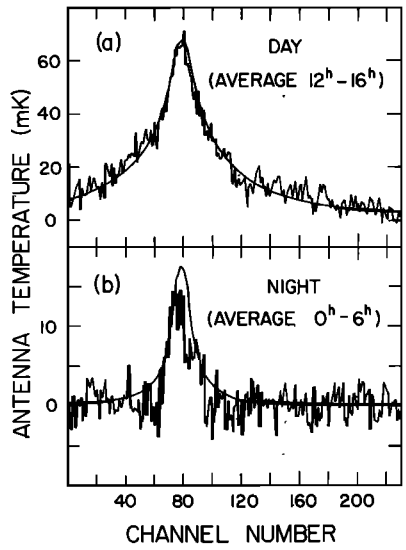

Fig. 16. (*a*) Average December 1982 ClO microwave data of *Solomon et al.* [1984] plotted as antenna temperature (millidegrees-K) versus channel number (1 MHz per channel); this is the rotational transition (J = 15/2 to 13/2) at 278.631 GHz. Data are averaged from 1200 to 1600 hours local time. Shown for comparison is a synthetic line profile (smooth curve) calculated with results of our December model averaged over the same local times and scaled down by a factor of 0.85. (*b*) Same as in (*a*), except for nighttime average (0000-0600 hours).

Our October model yields a peak column abundance almost 20% higher than in December, whereas the observations imply less ClO in October than in December. Again, seasonal variations are not necessarily well predicted by a one-dimensional model and changes in the radiation field alone; it remains to be seen how multidimensional models compare to these and future ClO observations. On the average these daytime microwave observations yield about 35% less ClO than our calculated values. This is not unreasonable, given the data uncertainties and the fact (discussed above) that our steady state model might indeed be overestimating the upper-stratospheric total chlorine abundance (2.6 ppbv instead of a more realistic value close to 2.0 ppbv).

We now focus on the relative diurnal variation observed by *Solomon et al.* [1984]. Their data are presented in Figure 17 in terms of an integrated intensity within ±50 MHz of the line center and are normalized to the observations in the 1200-1400 hour time bin. Two-hour averages for the whole set of October and December 1982 data are shown in parts *a* and *b*, respectively, of the figure. Reasonable uncertainties of ±20% (P. Solomon, private communication, 1983) have been assigned to each observation. The model diurnal variations in the ClO column above 31, 33, 35, and 37 km that are normalized to the noon values are shown for comparison to illustrate the sensitivity to the limits of integration. The main differences between these model curves are the slope of the decline near sunset and the ratio of maximum to minimum values during the 24-hour cycle. The diurnal variation in the model values for the column above 31 km appears to be the best match to the observed variation in the emission. At the higher altitudes there is less diurnal variation (see Figure 13), which is illustrated by the difference between the N_{31}^{∞} and N_{37}^{∞} model curves in Fig-

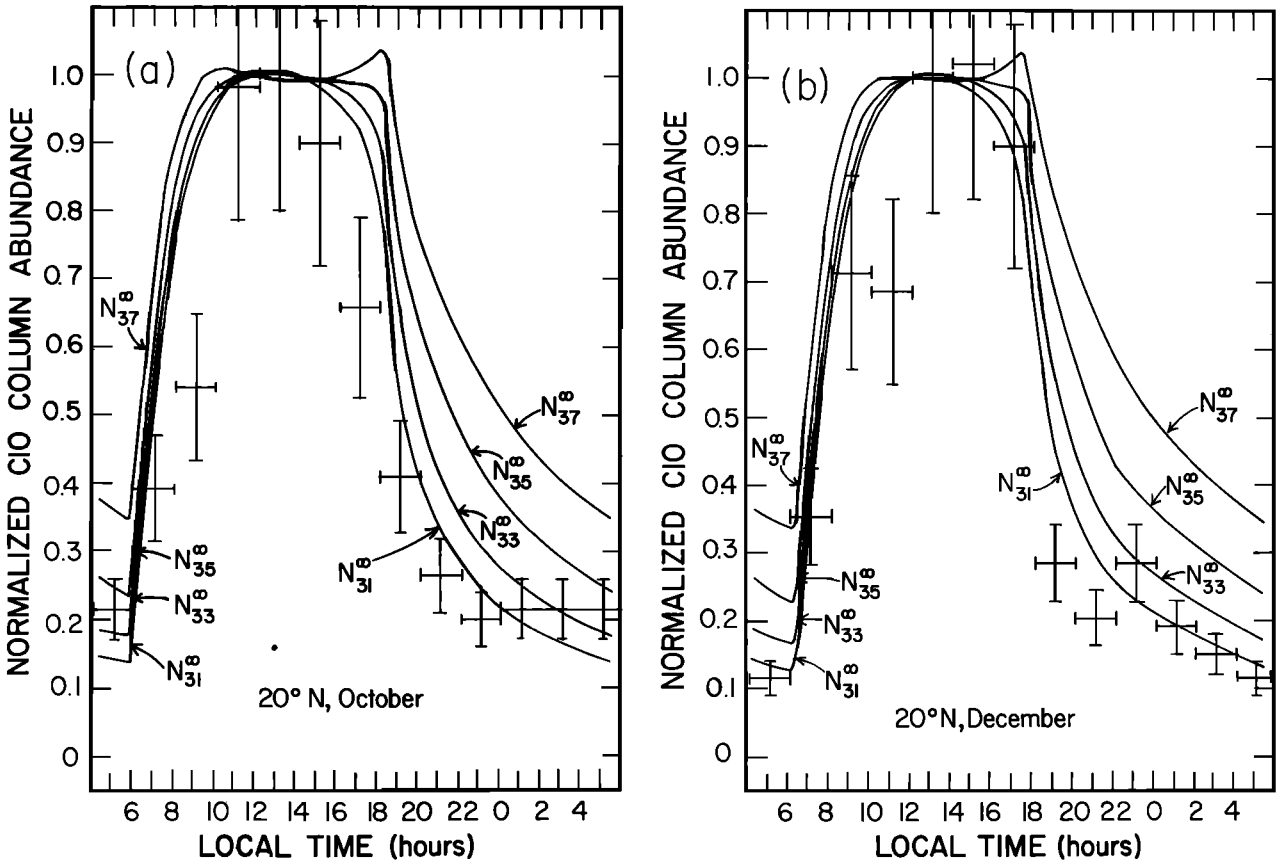

Fig. 17. (*a*) Comparison of averaged ground-based microwave observations of ClO diurnal variation obtained in October 1982 [*Solomon et al.*, 1984] with our model results; both are normalized to unity at noon. Data (with associated error bars) correspond to column abundances above about 30 km. Model column abundances above various altitudes are shown. (*b*) Same as in (*a*), except for December data and model values.

ure 17. Figure 18 shows the percent contributions to the total ClO column abundance as a function of time for various altitude ranges according to our model. During the day, most of the ClO resides between 30 and 40 km, while the 40-50 km range becomes dominant from about 10 P.M. to sunrise as a result of the smaller diurnal variation at those heights. This should show up as a narrowing of the observed ClO emission line during the evening and night, in addition to the decrease in intensity. Such a behavior is at least qualitatively observed in the data (P. Solomon, private communication, 1983).

The main discrepancy between our time-dependent model and ground-based microwave observations of ClO seems to be the somewhat faster calculated ClO increase after sunrise and possibly, although not as pronounced, the slower decrease in the afternoon. In particular the October observations between 0800 and 1000 hours local time are a factor of about 0.55 lower than the 1200-1400 hours peak values. This contrasts with the model ratio of about 0.9 and would seem to qualitatively agree with the slow morning increase in ClO abundances near 30 km observed between 0700 and 1000 hours by the balloon-borne microwave limb sounder (Figure 15). However, the December ground-based data near 0900 hours yield values of ~0.7, which persist into the 1000-1200 hours time bin. Differences between the data sets themselves also appear between 1600 and 1800 hours, when the October value of 0.65 is less in agreement with the model than the December value of 0.9. If the above differences between October and December are real, any model that can fit one set of data will probably not explain the other set. Further ground-based and balloon-borne observations will help define these apparent discrepancies between theory and measurements as well as provide an intercomparison between experiments. A decrease in the average model ClO amount available during the day can have an impact on the predicted catalytic destruction of ozone by chlorine radicals, which occurs mainly above 35 km, since the chlorine could be tied up in another "inert" reservoir, reducing the efficiency of the catalytic cycle. Based on the reasonable agreement between these observations and our model predictions, this potential effect should not be very large, unless it was due to some missing chemistry that also "short-circuited" the main ClO_x catalytic cycle.

Mumma et al. [1983] have attempted to detect ClO from the ground via laser heterodyne radiometer observations near sunset and sunrise. They obtain an upper limit for the column amount that is significantly lower than model predictions and the microwave observations discussed above. Given the noise in their data, the upper limit of a factor of 7 lower than previous daytime data seems somewhat high to us. In fact the above authors quote a factor of 5 difference, rather than 7, if a more subjective method is used to determine this upper limit (ClO line "just discerni-

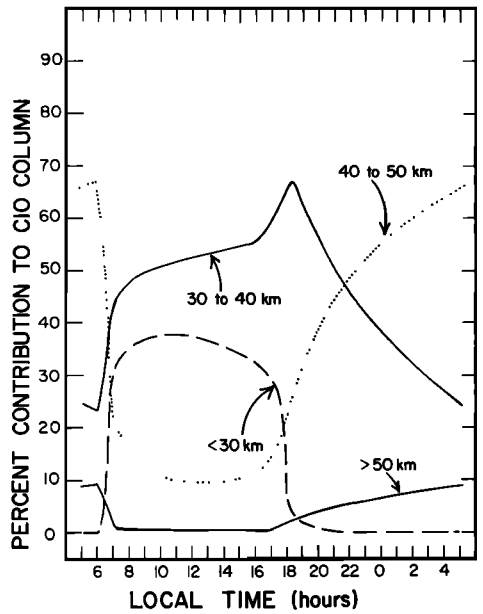

Fig. 18. Calculated percent contribution from various altitude ranges to the total model ClO column abundance as a function of time of day.

ble" in the residuals). Also, the infrared observations were conducted within an hour of sunset or sunrise. If one then considers the other data shown above, the early morning or late afternoon ClO abundances can be seen to differ from the noon values by as much as a factor of 2 (particularly in the morning). While this is not expected in terms of the models, it could, in reality, account for some of the difficulties associated with the infrared measurements. A factor of 2 or 3 difference between the latter "revised" upper limit and previous measurements of ClO is then less dramatic than a factor of 7, if one recalls also that the in situ data of *Anderson et al.* [1980] showed a spread about the mean by at least a factor of 2 or 3. On the other hand the ground-based microwave data do not exhibit such large variations from day to day or season to season (P. Solomon, private communication, 1984). Additional infrared observations from the ground and from balloon (or space) are needed in order to deal with the question of short-term variability.

The model diurnal changes in ClO (or ClO_x) result from the exchange between ClO_x radicals and $ClONO_2$. This can be seen from Figure 13 and a look at the mass balance for chlorine species as a function of time. Most of the diurnal variation in ClO occurs below about 40 km, where the abundance of $ClONO_2$ is comparable to or larger than the ClO abundance. Smaller variations occur in the uppermost stratosphere, where the absolute ClO concentration contributes little to the total column amount (except for late night and early morning, see Figure 18). The daytime photodissociation of $ClONO_2$ releases chlorine atoms to ClO_x and also HOCl. Except for times just after sunrise (within an hour of it), when HOCl photodissociation can contribute to the increase in [ClO], the dominant cause of diurnal changes in the ClO abundance is the exchange with $ClONO_2$ molecules. In the morning the formation of ClO is mainly a consequence of the photodissociation of $ClONO_2$, while the afternoon and sunset variations are primarily the result of the conversion from ClO to $ClONO_2$. Near 40 km and above, the smaller diurnal variation of ClO is in large part due to HOCl (and HCl), as shown in *Froidevaux* [1983] and *Ko and Sze* [1984].

Uncertainties in the absorption cross sections for both $ClONO_2$ and HOCl are apparently less than 5%-10% and the corresponding photodissociation rates in the stratosphere should be known to within 10%-20%, if one considers the fact that the fluxes and atmospheric transmission in the 300-400 nm range are well determined, particularly above 30 km. The rate of formation of HOCl involves a rate constant (k_{68}) that could be uncertain by up to 50%, but the ClO sensitivity to such a change is less than the sensitivity to $ClONO_2$-related uncertainties. The OH + HOCl reaction rate constant has not been measured and is a rough estimate [*DeMore et al.*, 1982], but since it is an order of magnitude less important than HOCl photodissociation in our current scheme, improvements in this reaction rate constant would either increase the total destruction rate of HOCl or leave it essentially unchanged, which will not help improve upon the possible discrepancies between models and observations of the ClO diurnal variation. The value for k_{66} (ClO + NO_2 + M reaction) is more critical, but the four available studies [see *DeMore et al.*, 1982] of this reaction show agreement within 20% of the mean for the pressure and temperature ranges of interest here. If we stretch the uncertainty in k_{66} by multiplying the current value by 1.50, we can indeed convert more ClO to $ClONO_2$, although the increase in $ClONO_2$ partially compensates in the morning by releasing more chlorine. In terms of the sunset observations of *Menzies* [1983] above 35 km, such a (diurnal) model sensitivity test leads to less than a 20% change in the ClO vertical gradient. The corresponding difference between our model and the above data is more than 50% and cannot be explained by the uncertainties in rate constants. The apparently low ClO column abundances above 30 km obtained by *Solomon et al.* [1984] near 9 or 10 A.M. are also difficult to account for, given the current uncertainties in photochemical data alone. The recent sensitivity analysis of the ClO diurnal variation by *Ko and Sze* [1984] corroborates this result; our predicted diurnal changes in chlorine species agree quite well with the above authors' calculations. Missing chemical cycles and possibly missing relatively stable chlorine reservoirs might have to be invoked in order to account for the above discrepancies, if real. The sensitivity to possible temperature changes (typically less than 10 K during the day at these altitudes) is not large enough either. In terms of NO_2, which recombines with ClO, we expect a smooth behavior during the day and no sharp impulse that could possibly modify the ClO variation near 9 A.M. We stress again that differences exist between the October and December microwave data that are as large as the discrepancies between our model and these observations. If real, such discrepancies could have important implications in terms of our understanding of the chlorine-related photochemical cycles as well as the net ozone destruction, and further detailed observational work (some of which is already in progress) should help define, if not explain, the existence of potential problems. Direct observations of both $ClONO_2$ and HOCl would, of course, be very useful. In summary the observed diurnal variation of ClO appears to be explainable by current theory to first order.

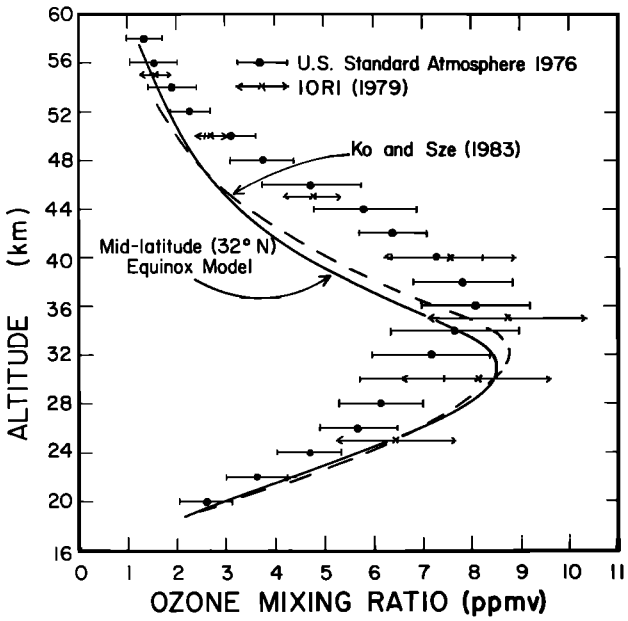

Fig. 19. Theoretical and observed mid-latitude ozone vertical profiles. The 30°N, equinox model of *Ko and Sze* [1983] is shown for comparison to our model. See text for description of data and error bars.

5. Model Ozone Deficit in the Upper Stratosphere

We now discuss an apparent discrepancy between the absolute concentration of upper stratospheric ozone calculated by our updated photochemical model and mean mid-latitude observations. This discrepancy of about 50% does not appear to be specific to our model and could have significant implications for our understanding of present and future ozone concentrations. Indeed, this problem exists even though, as shown earlier in this paper, the model compares favorably with the existing (average) observational results for the key radicals currently thought to catalyze the destruction of odd oxygen in the upper stratosphere. Unlike most other species, ozone has been measured repeatedly by a wide variety of techniques; its abundance does not display significant seasonal change (less than 20%) at mid-latitudes, near 40 km. In addition we will show that, given the current uncertainties in photochemical data (considerably improved during the last few years) and measurements of other trace species, upper stratospheric ozone is not very sensitive to any single model input parameter or any given trace gas concentration. This comes from the fact that ozone depends on many photochemical processes and catalytic cycles in that altitude range and that no single variable overwhelmingly controls its concentration.

5.1. *Model Comparison with Observations of O and O_3*

Theoretical and observational vertical profiles of ozone are compared in Figure 19. The U.S. Standard Atmosphere 1976 follows the observations summarized by *Krueger and Minzner* [1976], most of which are from optical (250-320 nm) balloon and rocket measurements between 30 and 60°N latitude. The ± 1 σ range of variability is indicated. The accuracy in individual determinations of $[O_3]$ is 15%-20%, but the mean of these data and almost every single sounding [see also *Krueger*, 1973] yield upper-stratospheric ozone abundances higher than our typical (32°N latitude, equinox, CIRA 1972, April background atmosphere) mid-latitude model. The same holds for the results reported in *Hudson et al.* [1982] concerning the International Ozone Rocket Intercomparison (IORI), held between October 21 and November 4, 1979, which represents data obtained more recently by several types of sensors (optical, infrared and chemiluminescent). The standard deviation in this case (see Figure 19) relates to the intercomparison between various instruments flown nearly simultaneously, with typically three flights for each instrument, as opposed to the U.S. Standard Atmosphere 1976 estimate of ozone variability, which to some extent includes daily, seasonal, and yearly variations. The model results (30°N latitude, equinox) of *Ko and Sze* [1983] are also shown for comparison in Figure 19. In the upper-stratospheric region, where disagreement between theory and data exists and where the model ozone is in photochemical equilibrium, the two models agree to within a few percent. This should be the case, since both models are using similar photochemical data (mostly from *DeMore et al.* [1982]) and reduced O_2 absorption cross sections (see model B of *Ko and Sze* [1983]).

Such a discrepancy between calculations and observations of upper stratospheric ozone has been noted in the past, as in the sensitivity study of *Butler* [1978] and the analysis of ozone data in the tropical [*Frederick et al.*, 1978] and high-latitude [*Frederick*, 1980] regions as well. Recent changes in input model parameters (decrease in $\sigma(O_2)$ in Herzberg continuum, increase in rate constant for $O + HO_2$ reaction) have further reduced the calculated ozone values in the upper stratosphere. The two upper-stratospheric model ozone profiles shown in Figure 19 agree very well (within $\pm 7\%$) with recent calculations for similar conditions (30°N latitude, equinox, U.S. Standard Atmosphere 1976 background atmosphere) by D. Wuebbles (private communication, 1984) and J. Herman (private communication by R. Stolarski, 1984). *Crutzen and Schmailzl* [1983] find an even larger discrepancy at mid-latitudes in the upper stratosphere. *Frederick et al.* [1984] show that the upper stratospheric mid-latitude ozone data obtained by the solar backscatter ultraviolet (SBUV) instrument on the Nimbus 7 satellite are systematically higher (by a factor of 1.2-1.6) than model results and, moreover, that the observed seasonal behavior (phase) is also in some disagreement with calculations. The extent to which the ozone discrepancy reaches into the mesosphere is not clear. The lower limits of the data in Figure 19 are close to our model values, but the relative variability becomes larger in the mesosphere. *Solomon et al.* [1983] have found that their mesospheric model results are somewhat low, compared to Solar Mesosphere Explorer (SME) ozone observations. The analysis of *Allen et al.* [1984] shows that reasonable agreement can be found between the Caltech mesospheric model and observations in the mesosphere, given the combined uncertainties in the measurements and the prescribed model parameters. However, this model did not include the effect of NO_x and ClO_x radicals, which would tend to reduce the predicted ozone concentrations by 10%-15% below about 55 km.

The mid-latitude data shown in Figure 19 are representative of the large number of observations collected until now by various groups using both in situ and remote sensing instruments. Other observations at mid-latitudes almost invariably fall within the limits shown in the above figure.

This is true, for example, for the OGO 4 BUV data [*London et al.*, 1977] as well as for the more recent SME satellite observations [*Rusch et al.*, 1983], the measurements from the satellite sensor SAGE (Stratospheric Aerosol and Gas Experiment) described by *Reiter and McCormick* [1982], and typical results from the Limb Infrared Monitor of the Stratosphere (LIMS) experiment on Nimbus 7 [*Remsberg et al.*, 1984]. The balloon-borne measurements presented by *Mauersberger et al.* [1981] also show a similar trend, although they apply mostly to altitudes below 38 km. Observed upper stratospheric seasonal variations are generally ±10%-20% at mid-latitudes, as demonstrated by *De Luisi et al.* [1979], *McPeters* [1980], *Prather* [1981], *Frederick et al.* [1983, 1984], and *McPeters et al.* [1984]. Ozone is quite sensitive to temperature [see also *Krueger et al.*, 1980], as discussed further below, and the seasonal variations are largely driven by changes in the solar radiation and temperature fields. In summary, considering the typical measurement uncertainties of less than 20%, the variety of techniques used, and the small seasonal (and diurnal) variations observed, the mean observed ozone abundances in the upper stratosphere are in disagreement with our model results and the majority of other recent calculations using the recommended photochemical input parameters. Clearly, more detailed comparisons with data sets involving simultaneous measurements of O_3, temperature, and other related species are needed, as well as a better understanding of differences between models themselves, in order to constrain the magnitude of the ozone discrepancy.

Given the above discrepancy in upper stratospheric ozone and the expected rapid chemical exchange between atomic oxygen and ozone within the odd oxygen family, it would be interesting to look for a possible discrepancy in the atomic oxygen concentration as well. In other words, if the ratio of [O] to [O_3] is as predicted from photochemical theory, we would expect to observe a higher than predicted absolute concentration of atomic oxygen in the upper stratosphere. There exists one experiment [*Anderson*, 1980] during which both ozone and atomic oxygen were measured simultaneously from a balloon flight above Palestine, Texas (32°N latitude, 2 December 1977). The resonance fluorescence atomic oxygen observations (smoothed profile sampled every 2 km with ±25% uncertainties) are compared to our model (32°N, equinox) in Figure 20*a*. As shown also in *Anderson* [1980], there is good agreement between the slope and magnitude of the [O] measurements and model results; note, however, that observed individual profiles (not shown here) show small scale structure as large as a factor of 2 in some cases. The ozone observations obtained with the Johnson Space Center Dasibi instrument in conjunction with the atomic oxygen data presented above, are displayed in Figure 20*b* along with our ozone model and other data shown previously in Figure 19. The similarity between the Dasibi ozone data and our model profile is striking, which leads to excellent agreement [see also *Anderson*, 1980] between the only existing measurement of [O]/[O_3] and the expected ratio in the stratosphere:

$$R_o = \frac{[O]}{[O_3]} = \frac{j_3 + j_4}{k_1[O_2][M]} \quad (6)$$

However, the fact that this particular ozone profile departs from the generally observed behavior above 35 km, in a way very similar to current photochemical theory, is anomalous. The ozone intercomparison shown in *Hudson et al.* [1982] suggests that upper stratospheric ozone measurements obtained by Dasibi instruments are lower than other data by as much as 30%. In fact the JSC Dasibi instrument is known to have been subject to such a systematic error (increasing at higher altitudes) prior to 1979, as discussed in *Mauersberger et al.* [1981]. Given the lim-

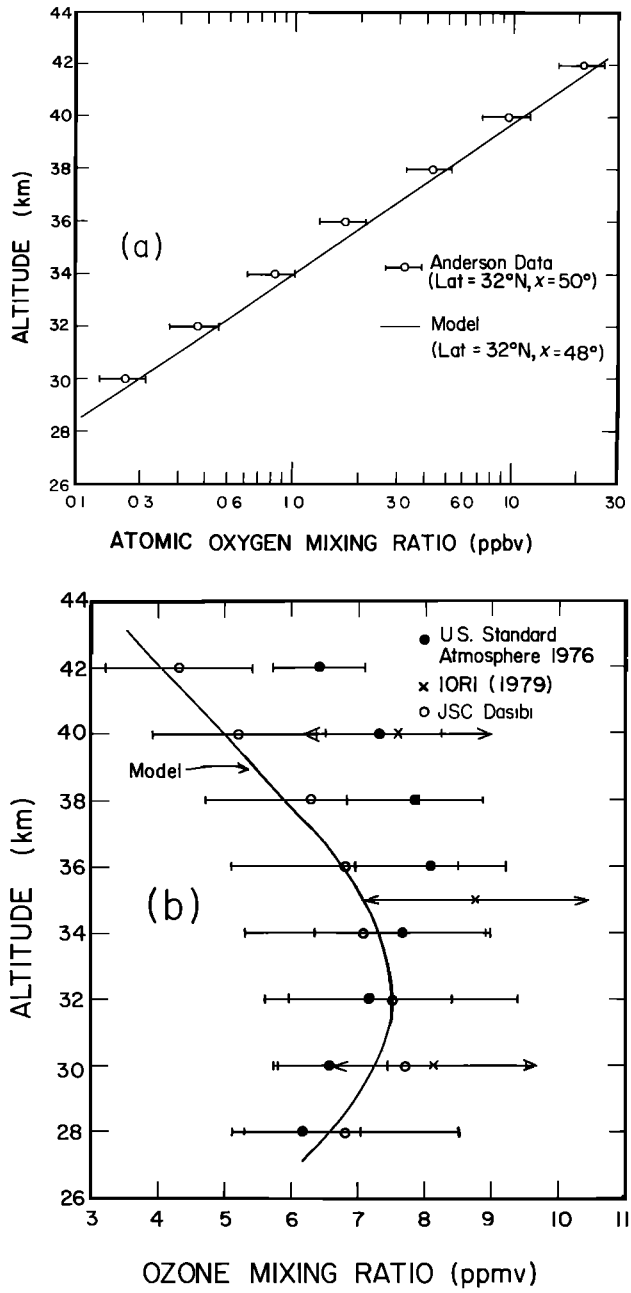

Fig. 20. (*a*) Atomic oxygen resonance fluorescence observations of *Anderson* [1980], taken on December 2, 1977 and compared to our standard model (32°N, -11° solar declination, CIRA 1972, April background atmosphere) for a similar solar zenith angle. We have smoothed the data between 30 and 42 km and sampled every 2 km. (*b*) Ozone data taken by Johnson Space Center Dasibi instrument of D. E. Robbins simultaneously with atomic oxygen data shown in (*a*) are shown by open circles. Our model and other data shown previously in Figure 19 are also plotted for comparison.

ited number of determinations of the ratio $[O]/[O_3]$ and these systematic errors, the apparent agreement between this measured ratio [*Anderson*, 1980] and theoretical results should thus be taken with caution. If the actual ozone values at the time of this experiment were close to the U.S. Standard Atmosphere 1976 values, it could be that the real value of $[O]/[O_3]$ is lower than model predictions by as much as 30%-50%. As discussed further below, this would affect the model destruction of odd oxygen and could account for much of the ozone discrepancy in the upper stratosphere. More evidence is needed in order to ascertain the value of this important ratio in the upper stratosphere, and we strongly recommend that this "pure O_x" system be further tested by detailed comparisons between models and observations.

5.2. *Model Sensitivity and Uncertainties*

We now address the possible model uncertainties that could help resolve the upper stratospheric ozone discrepancy. The various photochemical cycles affecting ozone have been extensively discussed elsewhere. Clearly, pure oxygen chemistry cannot fully describe the ozone concentrations in the stratosphere [e.g., *Nicolet*, 1975a; *Johnston*, 1975]. *Solomon et al.* [1980] further tested the global ozone balance by including losses caused by NO_x chemistry. A complete description of ozone (particularly in the upper stratosphere) should include losses due to all four catalyzing radical groups (O_x, NO_x, ClO_x, and HO_x). *Johnston and Podolske* [1978] have considered in great detail the various production and loss mechanisms for odd oxygen and conclude that the net destruction of ozone in the stratosphere is dominated by six or seven chemical reactions that take part in catalytic cycles. In photochemical steady state the balance between those processes that produce or destroy (via catalytic cycles) two odd oxygen species can be written as

$$\text{Prod}(O_x) = \text{Loss}(O_x)$$
$$= L(O_x) + L(HO_x) + L(NO_x) + L(ClO_x) \quad (7a)$$

where

$$\text{Prod}(O_x) = 2j_1[O_2] \quad (7b)$$

$$L(O_x) = 2k_2[O][O_3] \quad (7c)$$

$$L(HO_x) = 2\{k_{18}[O][HO_2] + k_{20}[O_3][HO_2] + k_{22}[O_3][H]\} \quad (7d)$$

$$L(NO_x) = 2k_{32}[O][NO_2] \quad (7e)$$

and

$$L(ClO_x) = 2k_{55}[O][ClO] \quad (7f)$$

The predicted importance of these various destruction rates, averaged over one diurnal cycle (essentially no production or loss at night, however), is shown as a percentage of $\text{Prod}(O_x)$ in Table 2, for altitudes between 32 and 48 km at 32°N latitude (standard model). These results are similar to the values shown in *Hudson et al.* [1982], but the importance of the chlorine cycle is higher in our model. Although destruction by NO_x dominates below 40 km, all four loss processes are seen to play a nonnegligible role in the 40-50 km range, where significant differences exist between observed and theoretical ozone profiles. An explicit equation for ozone in terms only of long-lived species is not readily inferred for the stratosphere, whereas the simpler mesospheric O_x -HO_x system lends itself more easily to such a relationship [*Allen et al.*, 1984]. A partial test of the ozone photochemical balance equation was made by *Anderson* [1980], but all the radical concentrations necessary for a meaningful test have not yet been satisfactorily and simultaneously measured.

Solutions to the ozone abundance problem could, in principle, involve one or more of the following (not entirely independent) answers: (1) The current photochemical laboratory data are sufficiently uncertain as not to preclude typical observed mid-latitude ozone profiles. (2) Some of the calculated radical concentrations affecting ozone, and maybe also the abundances of longer-lived species related to these radicals, are not in good agreement with average daytime observations. This might be related to 1 in terms of photochemical parameters, or it could arise from an inadequate representation of transport processes. (3) The model

TABLE 2. Relative Importance of Odd-Oxygen Destruction Rates

z, km	$L(O_x)$	$L(HO_x)$	$L(NO_x)$	$L(ClO_x)$
32	10	7	59	15
36	12	8	53	24
40	15	15	36	34
44	19	32	17	31
48	19	55	7	18

Numbers represent percentages relative to $\text{Prod}(O_x)$ and have been averaged over a diurnal cycle.

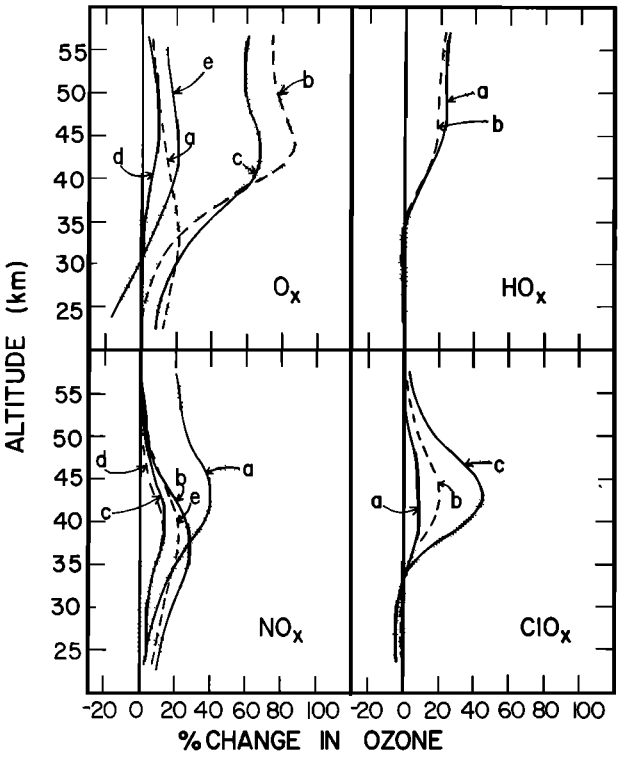

Fig. 21. Model tests (steady state diurnal average runs) of the ozone sensitivity to various photochemical parameters classified according to O_x, HO_x, NO_x, and ClO_x terms. The percent ozone increases necessary to fit the upper and lower bounds of the U.S. Standard Atmosphere 1976 O_3 data are indicated by the shaded area. Labeled curves represent the effect on ozone concentrations of individual changes in model parameters, as indicated below and discussed in the text. O_x: (*a*) j_3 ($O_3 \rightarrow O_2 + O$)/2; (*b*) j_4 ($O_3 \rightarrow O_2 + O(^1D)$)/2; (*c*) k_1 ($O + O_2 + M$) × 2; (*d*) k_2 ($O + O_3$)/2; (*e*) old σ (O_2). HO_x: (*a*) k_{18} ($O + HO_2$) × 2; (*b*) k_{29} ($OH + HO_2$) × 2 or $[H_2O]/2$. NO_x: (*a*) k_4 ($O(^1D) + O_2$) × 2 and k_5 ($O(^1D) + N_2$) × 2; (*b*) k_{32} ($O + NO_2$)/2; (*c*) k_{33} ($O_3 + NO$)/2; (*d*) j_9 (NO_2) × 2; (*e*) k_{10} ($O(^1D) + N_2 \rightarrow 2NO$)/2. ClO_x: (*a*) k_{55} ($O + ClO$)/2; (*b*) [ClO]/2; (*c*) no chlorine species.

description is lacking a significant "ingredient." We note that any postulated solution that significantly affects ozone in the right way should be regarded with caution if it produces a disagreement in other stratospheric gases or if it significantly worsens the mesospheric ozone profile fit.

To explore the effects of changes in adopted parameters, we have performed sensitivity tests with our mid-latitude (32°N) spring equinox model. Diurnally averaged steady state results are shown in Figure 21 in terms of the percent increase in ozone abundance arising from a change in input photochemical data; the upper and lower bounds required to fit the limits of the U.S. Standard Atmosphere 1976 O_3 profile are indicated as the limits of the shaded region. We typically change a parameter by a factor of 2 (increase or decrease); diurnal average tests, although economical, are not exactly accurate, but these are mainly intended to give us a reasonable idea of the sensitivity to various model changes. No single kinetic or photodissociation rate constant shown in the figure is as uncertain as a factor of 2, even at the lower stratospheric temperatures (except, perhaps, for the $OH + HO_2$ reaction), and we are merely showing how difficult it is to significantly change the ozone abundance with even unrealistically high variations in input data. Halocarbon source concentrations were held fixed in these tests. We have separated the changes in predicted ozone abundance due to parameters related primarily to O_x, HO_x, NO_x, and ClO_x, as indicated in the figure caption.

In the O_x category the rate constant k_1($O + O_2 + M$ reaction) affects ozone formation, and Figure 21 shows that $[O_3]$ is quite sensitive to its value. However, the change in k_1 necessary to fit the mean ozone data is unrealistically high, given the agreement (within ~20%) between various laboratory studies [*DeMore et al.*, 1982, and references therein]; this would also imply undesirably high mesospheric ozone values [see also *Allen et al.*, 1984]. Simultaneous observations of O and O_3 would bear directly on the value of k_1 (see expression (6)). A decrease in k_2($O + O_3$ reaction) reduces the effectiveness of the direct loss channel for O_x, but even a large change will not significantly increase $[O_3]$, since the total destruction rate depends only to a small extent on $L(O_x)$ (see Table 3). The photodissociation rate of O_3 will obviously play a role in controlling the ozone abundance and Figure 21 illustrates the sensitivity to j_3 ($O_3 + h\nu \rightarrow O_2 + O$) and j_4 ($O_3 + h\nu \rightarrow O_2 + O(^1D)$). The difference in the effects of a decrease in j_3 or j_4 is due to two factors: j_4 is sensitive to wavelengths short of 310 nm and dominates over j_3 above about 35 km, and a reduction in j_4 will also decrease the $O(^1D)$ concentration, which in turn reduces HO_x, NO_x, and ClO_x abundances and the efficiency of these catalytic cycles. The combination of smaller j_4 and smaller O_x destruction results in large $[O_3]$ increases, while a change in j_3 is not significant for upper stratospheric ozone. It should be emphasized that the O_3 absorption cross sections are known quite accurately from laboratory data, and we feel that the photodissociation rate of ozone in the upper stratosphere is known to better than 15%. Finally, one could go back to the old absorption cross sections $\sigma(O_2)$, which is equivalent to the effect of a significant (20%) increase in j_1 in the upper stratosphere. This effect alone, however, is not enough to eliminate the ozone discrepancy, and all of the recent O_2 cross section determinations point to values consistent with the low values used here [see also *Cheung et al.*, 1984; *Johnston et al.*, 1984].

Figure 21 shows a few examples of the ozone sensitivity to the HO_x radicals. The production of HO_x occurs via $O(^1D)$ reaction with H_2O, while the primary loss process at altitudes above 35 km is through the $OH + HO_2$ reaction. The ratio of [OH] to $[HO_2]$ depends to first order on four reactions [see, for example, *Hudson et al.*, 1982] and can be written as

$$\frac{[OH]}{[HO_2]} = \frac{k_{18}[O] + k_{34}[NO]}{k_{17}[O] + k_{19}[O_3]} \tag{8}$$

It is possible that our calculated H_2O abundance (6-7 ppmv) between 35 and 50 km is somewhat high for a mid-latitude average; a decrease by a factor of 2 in $[H_2O]$ produces changes similar to the effect of a factor of 2 increase in k_{29}($OH + HO_2$ reaction) by reducing $[HO_x]$ by 30%-40%. The effect of a decrease in k_{18}($O + HO_2$ reaction), which appears in (8) and has recently been revised upward by about 60% (see subsection 3.1), is also shown in Figure 21 [see also *Ko and Sze*, 1983]. Similar changes in other rate constants affecting HO_x concentrations will produce varia-

tions of order 20% or less in $[O_3]$. Large changes in individual rate constants would be needed to satisfy the ozone observations, and since HO_x is the primary component affecting mesospheric O_x, one has to reconcile possibly large effects on stratospheric ozone with even larger changes in mesospheric ozone. Moreover, necessary reductions in model HO_x by a factor of 2 or more (to significantly increase $[O_3]$) would not be consistent with currently existing observations of OH and HO_2.

The $O(^1D)$ concentration, although very small, is a key variable affecting the HO_x, NO_x, and ClO_x stratospheric abundances. Since NO_x is the main ozone-destroying component in most of the stratosphere, we have shown the effect of a reduction in $[O(^1D)]$ (by about a factor of 2) in the NO_x segment of Figure 21. This reduction is achieved by increasing the quenching rate of $O(^1D)$ by a factor of 2 (rate constants k_4 and k_5). A significant (up to 40%) increase in ozone results, but the real uncertainty in the above rate constants appears to be less than 20% [*DeMore et al.*, 1982]. The production rate of $O(^1D)$ through ozone photolysis is about as uncertain as its destruction rate, and unless an unknown mechanism exists in the atmosphere to deplete the $O(^1D)$ abundances (assuming that the 30%-40% resulting changes in HO_x, NO_x, and ClO_x concentrations are acceptable), the ozone discrepancy cannot be explained by such uncertainties. It is unfortunate that there is little hope of detecting $O(^1D)$ in the stratosphere at this time. To first order, in the upper stratosphere the $L(NO_x)$ term in (7) can be written using

$$k_{32}[NO_2] = \frac{k_{32}[NO_x]}{1 + ((j_9 + k_{32}[O])/k_{33}[O_3])} \quad (9)$$

where $[NO_x]$ is the sum of NO and NO_2 concentrations. The ozone sensitivity to the various parameters (k_{32}, k_{33} and j_9) in (9) is not very large in the upper stratosphere. In this case, large ozone changes above 40 km would have to be accompanied by larger changes in the 30-40 km range. The same holds for the 30%-40% reduction in $[NO_x]$ caused by dividing $k_{10}(N_2O + O(^1D)$ reaction) by 2.

Finally, the effect of changes in chlorine radicals cannot by itself produce the necessary ozone increase, although the variation with altitude qualitatively matches the required changes, as illustrated in Figure 21. The rate of importance here is $k_{55}[O][ClO]$. A decrease in k_{55} has a smaller effect on $[O_3]$ than a similar decrease in [ClO], as shown by cases *a* and *b* in the figure. This is due to the partially compensating increase in [ClO] caused by a decrease in k_{55}. Even if no chlorine species are included in our model, the mean ozone data are still high compared to theoretical values.

The uncertainties in rate constants or photodissociation rates of importance to ozone in the upper stratosphere are typically within 20%-40% (much less than a factor of 2). The above analysis indicates that no single change in the relevant photochemical data can, given the current uncertainties, increase the ozone abundance by more than 20% (much less in most cases). One would need to change several rate constants to get the required effect. An example in which four important reaction rate constants are changed by ±30% in a way to increase the ozone abundance is shown in Figure 22. It turns out that the O + ClO reaction (R55) has recently been studied in more detail (see subsection 4.1) and that a reduction in k_{55} by as much as 30% might indeed be indicated. Taken alone, however, this change affects $[O_3]$ by 5% or less. We do not find it satisfactory to suggest that small (15%) changes in six to ten reaction rate constants (or photodissociation rates) can explain the observed ozone concentrations. Figure 22 also illustrates the large ozone sensitivity to temperature changes. This follows from the temperature dependences of the O + O_2 + *M* and O + O_3 reactions, which both tend to increase ozone (primarily the latter reaction) if the temperature decreases. However, a systematic 20-30 K difference between our model temperatures and the actual stratospheric values is not likely, given that model values are obtained from observations with uncertainties of less than 5 K, in general. The range in the observed ozone data can probably, in large part, be explained by temperature changes, but we do not have the freedom to vary the temperature very much for mean mid-latitude model results. Similarly, the use of different background atmospheres for mid-latitudes can lead to changes in the model ozone values similar in magnitude to the seasonal changes of ±10%-15% observed at a given altitude in the upper stratosphere, but it is difficult to produce a much larger change for reasonable background atmospheres.

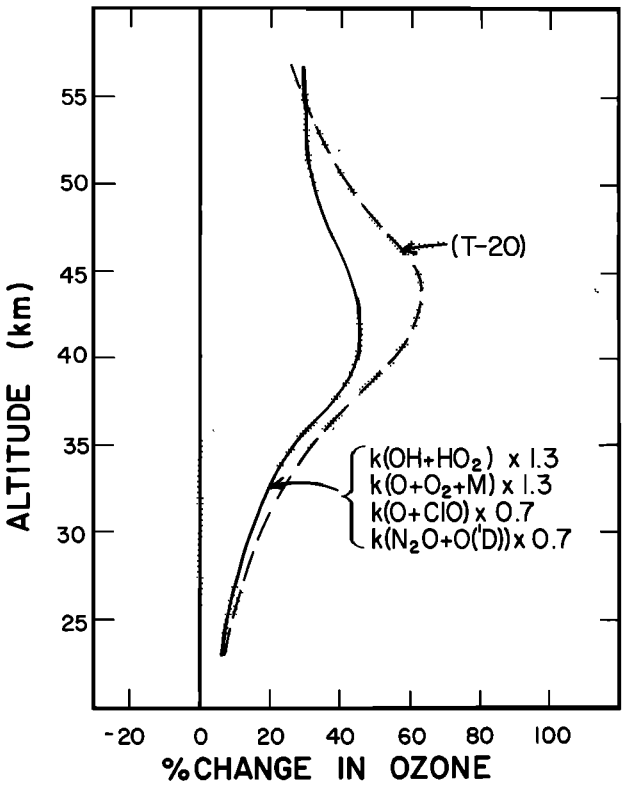

Fig. 22. Ozone sensitivity to a combination of ±30% changes in four rate constants chosen to increase $[O_3]$. Also shown is the separate effect of a 20° decrease in temperature. Shaded area has same meaning as in Figure 21.

We have had limited success in identifying one or two uncertain photochemical input parameters that could help resolve the discrepancy in upper stratospheric ozone. Furthermore, the observations of key radical concentrations presented in previous sections show reasonably good (within 20%-30%) overall agreement with our model results. We do

not find that our model yields a significant overestimate of mid-latitude HO_x, NO_x, or ClO_x abundances, but the accurate simultaneous observations necessary to fully test the ozone photochemical balance have not yet been satisfactorily performed. The concentrations of O and $O(^1D)$ play an important role in the ozone balance, and in fact the largest changes in $[O_3]$ shown in Figure 21 are related to changes involving the [O] to $[O_3]$ ratio (cases *b* and *c* in the O_x part of the figure) and the $O(^1D)$ abundance (case *a* in the NO_x part of the figure). Given the fact that the only existing measurement of $[O]/[O_3]$ below 42 km was not conclusive and quite likely lower than model predictions by 30%-50%, an amount consistent with the model/observation ozone discrepancy discussed here, we stress the importance of a more accurate determination of the ratio of atomic oxygen to ozone abundances in the upper stratosphere. In other words, given observations of $[O_3]$ along with [O], will the measured atomic oxygen concentration profile appear too low compared to theoretical expectations based on the measured $[O_3]$ and the predicted ratio of [O] to $[O_3]$? Since this ratio depends only on two model parameters (the total O_3 photodissociation rate constant $j_3 + j_4$ and the rate constant k_1), accurate measurements of O and O_3 would represent a crucial test of the presently accepted values of these key parameters. In terms of the $O(^1D)$ concentration (not measured in the stratosphere) it seems that a decrease from the predicted abundance by a factor larger than 2 would be required to account for the observed ozone abundances. This would significantly affect the predicted concentrations of HO_x, NO_x, and ClO_x radicals besides generating the difficulty of understanding how (as for the $[O]/[O_3]$ case) such a change would be produced.

Rather than attempting to find a way to reduce the photochemical destruction of ozone, can we enhance its production? The molecular oxygen photolysis rate, which is the source of odd oxygen, is somewhat uncertain because of the problems associated with the O_2 absorption cross section measurements in the Herzberg continuum. Uncertainties in j_1 of up to 25% currently exist in the upper stratosphere, with much higher uncertainties (of opposite sign) in the lower stratosphere. However, recent evidence indicates the need for a reduction in cross section, and a corresponding decrease in $[O_3]$, as discussed above. In terms of other possible sources of odd oxygen in the stratosphere, the evidence--and speculation--is limited. One possible mechanism involving an asymmetric $ClOO_2$ complex was proposed by *Prasad* [1980] in relation to the lower-than-observed stratospheric ClO abundances predicted by earlier models. Briefly, the idea involves the possible decomposition of $ClOO_2$ (formed by $ClO + O_2 + M$) into OClO + O, with subsequent photolysis of OClO into ClO + O. This process would thus break the O_2 bond and form odd oxygen. Only limited laboratory evidence exists regarding the above speculative scheme [see *DeMore et al.*, 1982; *Zellner and Handwerk*, 1982]. Moreover, even if we assume somewhat extreme rate constants and $ClOO_2$ abundances near 40 km in order to provide a significant odd oxygen source, we find unrealistically high (much higher than [ClO]) $ClOO_2$ concentrations near 30 km. This scheme, as it stands, does not seem to be plausible as a significant ozone source. Other possible sources of ozone could involve excited states of molecular oxygen (formed for example by the $O + O + M$ reaction) reacting with O_2 to form ozone. No quantitatively significant scheme has been found for the stratosphere. Finally, heavy molecular oxygen ($^{18}O^{16}O$) photodissociation might provide a source of odd oxygen in our atmosphere. Estimates of this source strength by *Cicerone and McCrumb* [1980] were fairly rough, and a recent detailed line by line calculation by *Blake et al.* [1984] yields only a few percent increase (at the most) in the odd oxygen production rate from heavy O_2.

The last question we consider is the possible role of transport in the upper stratospheric ozone distribution. Our one-dimensional model does not include an explicit description of transport processes, particularly meridional and zonal motions, which are typically much more rapid than vertical processes. Clearly, we cannot adequately simulate the latitudinal behavior of ozone or other long-lived species in the lower stratosphere, where horizontal motions dominate the photochemistry. Planetary scale waves (of low wave number) generated in the troposphere are thought to play a dominant role, notably during the winter, when they can propagate upward into the stratosphere and interact with the mean flow. Backscatter ultraviolet observations from satellites [*Heath et al.*, 1973; *London et al.*, 1977; *Frederick et al.*, 1977, 1980, 1983, 1984; *McPeters et al.*, 1984] have provided interesting global information on the ozone distribution and the influence of planetary waves. The question of importance for upper stratospheric ozone is the extent to which photochemical equilibrium is really valid. Observations (see references above) as well as models [e.g., *Cunnold et al.*, 1980; *Harwood and Pyle*, 1980] definitely point to dynamical control in the lower stratosphere, below 25 to 30 km. It is also generally agreed that above about 40 km, photochemistry will dominate. The coupling between radiation, chemistry, and dynamics (planetary waves) can lead to significant poleward and downward transport, according to the model of *Hartmann and Garcia* [1979], which yields a peak in horizontal transport near 45 km [see also *Hartmann*, 1981; *Rood and Schoeberl*, 1983]. Temperature-dependent reaction rates (for $O + O_3$, $O + O_2 + M$) lead to the coupling between photochemistry and temperature, which is in turn coupled to dynamical perturbations [*Pyle and Rogers*, 1980; *Strobel*, 1981]. The observed relationship between ozone and temperature perturbations in the upper stratosphere is generally an inverse relationship [*Barnett et al.*, 1975; *Ghazi et al.*, 1976; *Gille et al.*, 1980; *Nagatani and Miller*, 1984] in accordance with photochemical control. A direct relationship has been observed in the lower stratosphere [*Sreedharan and Mani*, 1973; *Gille et al.*, 1980]. Ghazi et al. note that even in the upper stratosphere (2-mbar pressure) there are instances where warm temperatures are accompanied by high ozone concentrations, as observed near 60°N latitude in January, indicating the influence of dynamical processes, possibly of the type discussed by *Hartmann and Garcia*. *Rood and Douglass* [1985] point out that the anticorrelation of ozone and temperature does not uniquely identify photochemical domination in the context of perturbations of the ozone concentration about the zonal mean. D. L. Hartmann (private communication, 1983) indicates that a purely photochemical model could underestimate the mean ozone abundance by as much as 15% near 40 km, although such differences will tend to occur mostly

at higher latitudes in the winter, where ozone gradients and planetary wave activity are larger. However, the mid-latitude ozone observations discussed here were not taken exclusively in the winter.

Crutzen and Schmailzl [1983] have recently discussed the apparent global imbalance between (annually averaged) ozone production (by O_2 photolysis) and loss rates calculated by using observed N_2O (source of NO_x radicals) and O_3 values in conjunction with model results for other species. In the lower stratosphere the production dominates the destruction. The situation in the upper stratosphere depends on the O_2 molecular cross section values. For the more plausible low values of $\sigma(O_2)$ the production is less than the loss of ozone above about 35 km, according to the above authors. They also calculate a lower-than-observed ozone concentration in the upper stratosphere (in fact, lower than our model predictions). It would be more satisfying to investigate the global ozone budget by a careful comparison of observations with a two-dimensional model for various latitudes (and altitudes) in order to determine where the imbalance actually occurs. A globally averaged analysis is subject to uncertainty in part because 90% of all ozone observations are for latitudes below 50° and that it is precisely in the region where total ozone peaks, at high latitudes in the winter, that the variability and uncertainties in the observations are largest. Further comparisons on a global scale, involving long-lived species such as N_2O, maybe CH_4, and also CF_2Cl_2, and $CFCl_3$, if possible, should be carried out in conjunction with ozone comparisons. It is tempting to argue for transport of ozone from the lower to upper stratosphere (if not directly vertically, maybe as a global redistribution), since this would smooth out the discrepancies in both lower- and upper-stratospheric regions and since the downward ozone fluxes are estimated and observed to be much smaller than needed to account for the lower stratospheric global imbalance. This, however, goes against the existing ideas related to transport time scales and the ozone photochemical lifetime in the upper stratosphere let alone the corresponding effects of such transport on other long-lived species, and we can offer no transport-related solution at this point.

Detailed observations of the diurnal behavior of ozone might also reveal unexpected trends if there is something missing in our model. The expected daytime variation of less than 10% below 50 km is difficult to accurately detect. Carefully planned broadband photometer rocket measurements of Hartley band absorption by *Lean* [1982] led to a precise determination of ozone daytime variations in the upper stratosphere and mesosphere. Approximate adjustments were made for independently measured temperature and density changes from night to day. The percent daytime changes in our model ozone concentrations agree quite well, in general, with the rocket results [*Froidevaux*, 1983]. A possible discrepancy occurs at 40 km, where the observed afternoon increase is about 13%, whereas our model result is close to 3%, in agreement with most current models. This difference might not seem large, but we find it difficult to explain if real [see *Froidevaux*, 1983, for further details]. It is also interesting and somewhat puzzling that an increase (from night to day) of close to 10% in O_3 near 30-35 km was seen by the LIMS instrument aboard Nimbus 7 [*Remsberg et al.*, 1984]. This systematic diurnal increase in zonal mean ozone (at constant pressure), observed at more than one latitude (J. Russell, private communication, 1983), appears to be real. The large abundance of ozone near 30 km makes it very difficult to produce such an increase, and our model predicts a 1%-2% change, at most. The observed increase by LIMS near 40 km, however, is close to 5%, in much better agreement with model results, and significantly less than the 13% increase obtained by *Lean* [1982]. The above data on daytime changes in stratospheric ozone are somewhat contradictory and uncertain, but we note that larger-than-expected increases would tend to substantiate the current discrepancy in the mean ozone abundance.

6. Conclusions

It is clearly necessary to understand the present state of the terrestrial atmosphere (dynamics and chemistry) if model predictions of future atmospheric changes are to become more reliable. In this paper we have discussed essential aspects of stratospheric chemistry affecting the distributions of ozone and key free radicals in the catalytic cycles that destroy ozone, notably ClO. Our updated photochemical model provides a reasonably good fit to average mid-latitude ClO data and observations of hydrogen and nitrogen oxides in the stratosphere. In fact, older chemistry is generally not as acceptable in terms of such observations (e.g., the slope and magnitude of the ClO profile, OH and HO_2 ground-based data, $[HNO_3]/[NO_2]$ ratio). The model comparison to diurnal ClO observations indicates at least first order agreement in terms of a breathing cycle with $ClONO_2$. However, certain discrepancies remain or have recently surfaced. Low ClO abundances at certain times (morning in particular) are hardly explainable in terms of uncertainties in the current photochemical data and might suggest an unknown chlorine reservoir or some missing chemistry. Such effects could reduce the efficiency of the chlorine catalytic cycle. Simultaneous observations of ClO and HCl at various altitudes would represent a significant step in our attempt to close the gap between models and observations.

Despite reasonable agreement between our model results and the average of existing observations of key radical species, the mean observed ozone abundance in the upper stratosphere is higher than predicted by about 50%. This is a systematic effect, apparent to some extent in virtually every observation, regardless of time of day or year, so that an underestimate of observational uncertainties does not seem to be a likely explanation. Such a discrepancy between observed and calculated upper-stratospheric and lower-mesospheric ozone has been noted by others in the past (as discussed above) but has been enhanced recently by changes in $\sigma(O_2)$ and $k(O + HO_2)$. At present, most modeling groups agree with the existence of a deficit in calculated upper-stratospheric ozone, although we need to refine the comparisons between high-quality data sets and models as well as between different models themselves. Moreover, a fairly accurate laboratory data base appears to have been established, so that it is not very easy to argue for large errors in any single rate constant or absorption cross section. Our sensitivity analysis essentially rules out the possibility of one or two large adjustments in the current photochemical scheme in order to fit the mean ozone observations in the upper stratosphere. While a combination of

many smaller adjustments could significantly reduce the discrepancy, we do not find that this satisfactorily eliminates the systematic difference between mean observations and theory. The photodissociation rate of O_2 is the major term for O_x production, but given the current uncertainties in absorption cross sections, there are still large uncertainties in the value of this key rate (particularly in the lower stratosphere). Recent indications would tend to lower $\sigma(O_2)$, thus allowing more flux in the lower stratosphere and also increasing the global production of ozone [see also *Crutzen and Schmailzl*, 1983]. This increase, however, would not manifest itself in the upper stratosphere, where a decrease in $\sigma(O_2)$ leads to a decrease in O_3, and it is difficult to see how transport processes could shift ozone from the lower to upper stratosphere given the short chemical lifetime of ozone above 35 km. Because of the one-dimensional nature of this model, we have emphasized the upper-stratospheric discrepancy in ozone, whereas Crutzen and Schmailzl focused on the global imbalance in the lower stratosphere (25-35 km), where models tend to overestimate the ozone concentration. We feel that there is more room for model uncertainties in the lower stratosphere as a result of transport (horizontal, in particular), the radiation field (higher optical depth implies more sensitivity to O_2 and O_3 cross sections), and the more complex chemical cycles. However, we do not disagree with the above authors that there are indications of an "extremely dissatisfactory state of affairs" in the ozone balance.

In the upper stratosphere the loss processes for odd oxygen are possibly being overestimated by models. We note that the $O(^1D)$ concentration is a key variable that could change the ozone concentration without affecting the predicted radical abundances in a drastic way (given the observational coverage and uncertainties), since three major ozone destruction mechanisms (by HO_x, NO_x, and ClO_x) are simultaneously affected; however, uncertainties in the known production and loss mechanisms for $O(^1D)$ are not large enough. We strongly favor new simultaneous measurements of atomic oxygen and ozone in order to isolate possible errors in the key model parameters affecting the $[O]/[O_3]$ ratio and in view of the limited and somewhat controversial nature of the only detection of this kind to date. In the next few years it seems likely that observational tests of the (local) ozone balance in the upper stratosphere will become feasible through careful monitoring of ozone, temperature, and the key radicals NO_2, HO_2, and ClO (and maybe also O, OH, and NO) during the daytime hours, from a balloon platform. Besides the accuracy needed in the measurements of these radical concentrations, one would also hope for somewhat smaller uncertainties in the corresponding laboratory data, since it is the product of rate constants and concentrations that determines the rate of ozone destruction. The uncertainties in $k_2(O + O_3)$, $k_{18}(O + HO_2)$, $k_{22}(O + NO_2)$, and $k_{55}(O + ClO)$ for upper stratospheric temperatures are currently about 30%, 40%, 10%, and 30%, respectively. Detailed measurements and comparisons with calculations of the solar flux in the middle and upper stratosphere at wavelengths between 180 and 320 nm would enable one to look for discrepancies in the UV radiation field that is responsible for the photodissociation of O_2 and O_3 as well as the production of stratospheric $O(^1D)$, HO_x, NO_x, and ClO_x radicals. In addition, such measurements as a function of season could give some clues regarding not only the question of the absolute O_3 concentration but also its associated seasonal phase as a function of height (see problems discussed by *Frederick et al.* [1984]).

In a general sense, more attention has to be paid to quality of observation and the associated increase in our knowledge of the atmosphere. *Harries* [1982] notes, for example, that tests of certain photochemical equilibrium relations can be made meaningful only with highly accurate simultaneous observations. The detection of new species, such as HO_2NO_2, HOCl, $ClONO_2$, or N_2O_5, would obviously increase the possibilities of comparing observations with models, which in that respect are ahead of the observations. Simultaneous observations are still of primary importance, and NASA is presently focusing more on joint balloon flights and intercomparisons between various measurement techniques. In other words, one more ClO profile is not nearly as important as a simultaneous detection of ClO and HCl, possibly by more than one or two instruments. Comparisons of multidimensional models with latitudinal variations of stratospheric gases will help further our understanding of chemistry, dynamics, and their interaction. A recent example concerns the global NO_x observations and analysis [*Noxon et al.*, 1983], coupled with two-dimensional model comparisons [*Solomon and Garcia*, 1983]. Despite the encouraging results, there are indications that some missing factors still exist in relation to the NO_x reservoirs at high latitudes.

The photochemical modeler is often faced with the dilemma of suggesting a possible change that will help reduce a certain discrepancy in a constituent's abundance while leaving other species in reasonable agreement with observations. This challenge represents a kind of Rubik's cube, and while we seem to have mostly the right colors on each side, there are still some unmatched, and maybe missing, spots. The current first-order agreement between models and observations can be satisfying, but we have to further refine the level of comparison if we are to believe predictions of small (but possibly important) column ozone depletion rates due to a variety of long-term trends in minor and trace gases.

Acknowledgments. This work was facilitated by discussions and communications (often in advance of publication) with many individuals. In this respect, we thank J. W. Birks, W. B. DeMore, R. L. de Zafra, P. Fabian, C. B. Farmer, J. E. Frederick, G. W. Kattawar, L. F. Keyser, M. T. Leu, J. J. Margitan, R. T. Menzies, M. J. Molina, S. S. Prasad, O. F. Raper, S. P. Sander, N. D. Sze, P. M. Solomon, and J. W. Waters. This research was supported by NASA grant NAGW-413.

Contribution 4011 of the Division of Geological and Planetary Sciences, California Institute of Technology.

REFERENCES

Adams, C. N., and G. W. Kattawar, Radiative transfer in spherical shell atmospheres, 1, Rayleigh scattering, *Icarus, 35*, 139-151, 1978.

Adams, C. N., G. N. Plass, and G. W. Kattawar, The influence of ozone and aerosols on the brightness and color of the twilight sky, *J. Atmos. Sci., 31*, 1662-1674, 1974.

Allen, M., and J. E. Frederick, Effective photodissociation cross sec-

tions for molecular oxygen and nitric oxide in the Schumann-Runge bands, *J. Atmos. Sci.*, *39*, 2066-2075, 1982.
Allen, M., Y. L. Yung, and J. W. Waters, Vertical transport and photochemistry in the terrestrial mesosphere and lower thermosphere (50-120 km), *J. Geophys. Res.*, *86*, 3617-3627, 1981.
Allen, M., J. I. Lunine, and Y. L. Yung, The vertical distribution of ozone in the mesosphere and lower thermosphere, *J. Geophys. Res.*, *89*, 4841-4872, 1984.
Anderson, Jr., D. E., The troposphere-stratosphere radiation field at twilight: A spherical model, *Planet. Space Sci.*, *31*, 1517-1523, 1983.
Anderson, G. P., and L. A. Hall, Attenuation of solar irradiance in the stratosphere: Spectrometer measurements between 191 and 207 nm, *J. Geophys. Res.*, *88*, 6801-6806, 1983.
Anderson, J. G., Free radicals in the earth's stratosphere: A review of recent results, Proceedings of the NATO Advanced Study Institute on Atmospheric Ozone: Its Variation and Human Influences, *Rep. FAA-EE-80-20*, pp. 233-251, U.S. Dep. Transp., Washington, D.C., 1980.
Anderson, J. G., R. E. Shetter, H. J. Grassel, and J. J. Margitan, Stratospheric free chlorine measured by balloon-borne in situ resonance fluorescence, *J. Geophys. Res.*, *85*, 2869-2887, 1980.
Anderson, J. G., H. J. Grassl, R. E. Shetter, and J. J. Margitan, HO_2 in the stratosphere: Three in situ observations, *Geophys. Res. Lett.*, *8*, 289-292, 1981.
Arnold, F., and S. Qiu, Upper stratosphere negative ion composition measurements and inferred trace gas abundances, *Planet. Space Sci.*, *32*, 169-177, 1984.
Ashby, R. W., A numerical study of the chemical composition of the stratosphere, Ph.D. thesis, pp. 302, Univ. Wis., Madison, 1976.
Bahta, A., R. Simonaitis, and J. Heicklen, Thermal decomposition kinetics of $CH_3O_2NO_2$, *J. Phys. Chem.*, *86*, 1849-1853, 1982.
Barnett, J. J., J. T. Houghton, and J. A. Pyle, The temperature dependence of the ozone concentration near the stratopause, *Q. J. R. Meteorol. Soc.*, *101*, 245-257, 1975.
Baulch, D. L., R. A. Cox, P. J. Crutzen, R. F. Hampson, Jr., J. A. Kerr, J. Troe, and R. T. Watson, Evaluated kinetic and photochemical data for atmospheric chemistry: Supplement 1, CODATA task group on chemical kinetics, *J. Phys. Chem. Ref. Data*, *11*, 327-496, 1982.
Blake, A. J., S. T. Gibson, and D. G. McCoy, Photodissociation of $^{16}O^{18}O$ in the atmosphere, *J. Geophys. Res.*, *89*, 7277-7284, 1984.
Blattner, W. G., H. G. Horak, D. G. Collins, and M. B. Wells, Monte Carlo studies of the sky radiation at twilight, *Appl. Opt.*, *13*, 534-547, 1974.
Boughner, R. E., A simplified method for the calculation of diurnally averaged photodissociation rates, *J. Atmos. Sci.*, *37*, 1308-1312, 1980.
Brasseur, G., A. De Rudder, and P. C. Simon, Implication for stratospheric composition of a reduced absorption cross section in the Herzberg continuum of molecular oxygen, *Geophys. Res. Lett.*, *10*, 20-23, 1983.
Brune, W. H., J. J. Schwab, and J. G. Anderson, Laser magnetic resonance, resonance fluorescence, and resonance absorption studies of the reaction kinetics of $O + OH \rightarrow H + O_2$, $O + HO_2 \rightarrow OH + O_2$, $N + OH \rightarrow H + NO$, and $N + HO_2 \rightarrow$ products at 300 K between 1 and 5 torr, *J. Phys. Chem.*, *87*, 4503-4514, 1983.
Burnett, C. R., and E. B. Burnett, Spectroscopic measurements of the vertical column abundance of hydroxyl (OH) in the earth's atmosphere, *J. Geophys. Res.*, *86*, 5185-5202, 1981.
Burnett, C. R., and E. B. Burnett, Vertical column abundance of atmospheric OH at solar maximum from Fritz Peak, Colorado, *Geophys. Res. Lett.*, *9*, 708-711, 1982.
Butler, D. M., The uncertainty in ozone calculations by a stratospheric photochemical model, *Geophys. Res. Lett.*, *5*, 769-772, 1978.
Callis, L. B., V. Ramanathan, R. E. Boughner, and B. R. Barkstrom, The stratosphere: Scattering effects, a coupled 1-D model, and thermal balance effects, paper presented at Fourth Conference on Clim. Impact Assessment Program, U.S. Dep. Transp., Washington, D.C., 1975.
Callis, L. B., M. Natarajan, and R. E. Boughner, On the relationship between the greenhouse effect, atmospheric photochemistry, and species distribution, *J. Geophys. Res.*, *88*, 1401-1426, 1983.
Chance, K. V., and W. A. Traub, An upper limit for stratospheric hydrogen peroxide, *J. Geophys. Res.*, *89*, 11,655-11,660, 1984.
Cheung, A. S.-C., K. Yoshino, W. H. Parkinson, and D. E. Freeman, Herzberg continuum cross section of oxygen in the wavelength region 193.5-204.0 nm: New laboratory measurements and stratospheric implications, *Geophys. Res. Lett.*, *11*, 580-582, 1984.
Cicerone, R. J., Halogens in the atmosphere, *Rev. Geophys*, *19*, 123-139, 1981.
Cicerone, R. J., and J. L. McCrumb, Photodissociation of isotropically heavy O_2 as a source of atmospheric O_3, *Geophys. Res. Lett.*, *7*, 251-254, 1980.
Cicerone, R. J., S. Walters, and S. C. Liu, Nonlinear response of stratospheric ozone column to chlorine injections, *J. Geophys. Res.*, *88*, 3647-3661, 1983.
Cogley, A. C., and W. J. Borucki, Exponential approximation for daily average solar heating or photolysis, *J. Atmos. Sci.*, *33*, 1347-1356, 1976.
Cox, R. A., J. P. Burrows, and G. B. Coker, Product formation in the association reaction of ClO with NO_2 investigated by diode laser kinetic spectroscopy, *Int. J. Chem. Kinet.*, *6*, 445-467, 1984.
Crutzen, P. J., and U. Schmailzl, Chemical budgets of the stratosphere, *Planet. Space Sci.*, *31*, 1009-1032, 1983.
Cunnold, D. M., F. N. Alyea, and R. G. Prinn, Preliminary calculations concerning the maintenance of the zonal mean ozone distribution in the northern hemisphere, *Pure Appl. Geophys.*, *118*, 329-354, 1980.
Dalgarno, A., Atmospheric reactions with energetic particles, *Space Res.*, *7*, 849-861, 1967.
DeLuisi, J. J., C. L. Mateer, and D. F. Heath, Comparison of seasonal variations of upper stratospheric ozone concentrations revealed by Umkehr and Nimbus 4 BUV observations, *J. Geophys. Res.*, *84*, 3728-3732, 1979.
DeMore, W. B., R. T. Watson, D. M. Golden, R. F. Hampson, M. J. Kurylo, C. J. Howard, M. J. Molina, and A. R. Ravishankara, Chemical Kinetics and Photochemical Data for Use in Stratospheric Modeling, Publ. 82-57, Jet Propul. Lab., Pasadena, Calif., 1982.
DeMore, W. B., M. J. Molina, R. T. Watson, D. M. Golden, R. F. Hampson, M. J. Kurylo, C. J. Howard, and A. R. Ravishankara, Chemical Kinetics and Photochemical Data for Use in Stratospheric Modeling, Publ. 83-62, Jet Propul. Lab., Pasadena, Calif., 1983.
de Zafra, R. L., A. Parrish, P. M. Solomon, and J. W. Barrett, A measurement of stratospheric HO_2 by ground-based millimeter-wave spectroscopy, *J. Geophys. Res.*, *89*, 1321-1326, 1984
Drummond, J. R., and R. F. Jarnot, Infrared measurements of stratospheric composition II. Simultaneous NO and NO_2 measurements, *Proc. R. Soc. London, A*, *364*, 237-254, 1978.
Ehhalt, D. H., and A. Tonnissen, Hydrogen and carbon compounds in the stratosphere, Proceedings of the NATO Advanced Study Institute on Atmospheric Ozone: Its Variation and Human Influences, *Rep FAA-EE-80-20*, pp. 129-152, U.S. Dep. Transp., Washington, D. C., 1980.
Evans, W. F. J., J. B. Kerr, D. I. Wardel, J. C. McConnell, B. A. Ridley, and H. I. Schiff, Intercomparison of NO, NO_2, and HNO_3 measurements with photochemical theory, *Atmosphere*, *14*, 189-198, 1976.
Evans, W. F. J., C. T. McElroy, and J. B. Kerr, Simulation of the October 23, 1980, Stratoprobe flight, *Geophys. Res. Lett.*, *9*, 223-226, 1982.
Feautrier, P., Sur la resolution numerique de l'equation de transfert, *C. R. Acad. Sci. Paris*, *258*, 3189-3191, 1964.
Fiocco, G., Influence of diffuse solar radiation on stratospheric chemistry, Proceedings of the NATO Advanced Study Institute on Atmospheric Ozone: Its Variation and Human Influences, *Rep. FAA-EE-80-20*, pp. 555-587, U.S. Dep. Transp., Washington, D.C., 1980.
Fishman, J., The distribution of NO_x and the production of ozone: Comments on "On the origin of tropospheric ozone," by S. C. Liu et al., *J. Geophys. Res.*, *86*, 12,161-12,164, 1981.
Fishman, J., and P. J. Crutzen, A numerical study of tropospheric photochemistry using a one-dimensional model, *J. Geophys. Res.*, *82*, 5897-5906, 1977.
Frederick, J. E., Seasonal variations in high-latitude ozone and

metastable molecular oxygen emissions: A theoretical interpretation, *J. Geophys. Res.*, *85*, 1611-1617, 1980.

Frederick, J. E., and R. D. Hudson, Predissociation linewidths and oscillator strengths for the (2-O) to (13-O) Schumann-Runge bands of O_2, *J. Mol. Spectrosc.*, *74*, 247-258, 1979.

Frederick, J. E., and R. D. Hudson, Dissociation of molecular oxygen in the Schumann-Runge bands, *J. Atmos. Sci.*, *37*, 1099-1106, 1980.

Frederick, J. E., and J. E. Mentall, Solar irradiance in the stratosphere: Implications for the Herzberg continuum absorption of O_2, *Geophys. Res. Lett.*, *9*, 461-464, 1982.

Frederick, J. E., B. W. Guenther, and D. F. Heath, Spatial variations in tropical ozone: The influence of meridional transport and planetary waves in the stratosphere, *Beitr. Phys. Atmos.*, *50*, 496-507, 1977.

Frederick, J. E., B. W. Guenther, P. B. Hays, and D. F. Heath, Ozone profiles and chemical loss rates in the tropical stratosphere deduced from backscatter ultraviolet measurements, *J. Geophys. Res.*, *83*, 953-958, 1978.

Frederick, J. E., R. B. Abrams, R. Dasgupta, and B. Guenther, An observed annual cycle in tropical upper stratospheric and mesospheric ozone, *Geophys. Res. Lett.*, *7*, 713-716, 1980.

Frederick, J. E., F. T. Huang, A. R. Douglass, and C. A. Reber, The distribution and annual cycle of ozone in the upper stratosphere, *J. Geophys. Res.*, *88*, 3819-3828, 1983.

Frederick, J. E., G. N. Serafino, and A. R. Douglass, An analysis of the annual cycle in upper stratospheric ozone, *J. Geophys. Res.*, *89*, 9547-9555, 1984.

Froidevaux, L., Photochemical modeling of the earth's stratosphere, Ph.D. thesis, pp. 275, Calif. Inst. Technol., Pasadena, 1983.

Froidevaux, L., and Y. L. Yung, Radiation and chemistry in the stratosphere: Sensitivity to O_2 absorption cross sections in the Herzberg continuum, *Geophys. Res. Lett.*, *9*, 854-857, 1982.

Gallagher, C. C., C. A. Forsberg, and R. V. Pieri, Stratospheric N_2O, CF_2Cl_2, and $CFCl_3$ composition studies utilizing in situ cryogenic, whole air sampling methods, *J. Geophys. Res.*, *88*, 3798-3808, 1983.

Ghazi, A., A. Ebel, and D. F. Heath, A study of satellite observations of ozone and stratospheric temperatures during 1970-1971, *J. Geophys. Res.*, *81*, 5365-5373, 1976.

Gidel, L. T., P. J. Crutzen, and J. Fishman, A two-dimensional photochemical model of the atmosphere, 1, Chlorocarbon emissions and their effect on stratospheric ozone, *J. Geophys. Res.*, *88*, 6622-6640, 1983.

Gille, J. C., P. L. Bailey, and J. M. Russell, III, Temperature and composition measurements from the LRIR and LIMS experiments on Nimbus 6 and 7, *Phil. Trans. R. Soc. London, Ser. A*, *296*, 205-218, 1980.

Gladstone, G. R., Radiative transfer with partial frequency redistribution in inhomogeneous atmospheres: Application to the Jovian aurora, *J. Quant. Spectrosc. Radiat. Transfer*, *27*, 545-556, 1982.

Goldan, P. D., W. C. Kuster, D. L. Albritton, and A. L. Schmeltokopf, Stratospheric $CFCl_3$, CF_2Cl_2, and N_2O height profile measurements at several latitudes, *J. Geophys. Res.*, *85*, 413-423, 1980.

Hampson, R. F., Chemical Kenetic and Photochemical Data Sheets for Atmospheric Reactions, *Rep. EE-80-17*, Fed. Aviat. Agency, Washington, D. C., 1980.

Hampson, R. F., and D. Garvin (eds.), Reaction Rate and Photochemical Data for Atmospheric Chemistry--1977, *NBS SP-513*, Nat. Bur. Stand., Washington, D.C., 1978.

Harries, J. E., Ratio of HNO_3 to NO_2 concentrations in the daytime stratosphere, *Nature*, *274*, 235, 1978.

Harries, J. E., Stratospheric composition measurements as tests of photochemical theory, *J. Atmos. Terr. Phys.*, *44*, 591-597, 1982.

Hartmann, D. L., Some aspects of the coupling between radiation, chemistry, and dynamics in the stratosphere, *J. Geophys. Res.*, *86*, 9631-9640, 1981.

Hartmann, D. L., and R. R. Garcia, A mechanistic model of ozone transport by planetary waves in the stratosphere, *J. Atmos. Sci.*, *36*, 350-364, 1979.

Harwood, R. S., and J. A. Pyle, The dynamical behavior of a two-dimensional model of the stratosphere, *Q. J. R. Meteorol. Soc.*, *106*, 395-420, 1980.

Heaps, W. S., and T. J. McGee, Balloone borne LIDAR measurements of stratospheric hydroxyl radical, *J. Geophys. Res.*, *88*, 5281-5289, 1983.

Heath, D. F., C. L. Mateer, and A. J. Krueger, The Nimbus-4 backscatter ultraviolet (BUV) atmospheric ozone experiment--Two years' operation, *Pure Appl. Geophys.*, *106-108*, 1238-1253, 1973.

Herman, J. R., and J. E. Mentall, O_2 absorption cross sections (187-225 nm) from stratospheric solar flux measurements, *J. Geophys. Res.*, *87*, 8967-8975, 1982.

Horvath, J. J., J. E. Frederick, N. Orsini, and A. R. Douglass, Nitric oxide in the upper stratosphere: Measurements and geophysical interpretation, *J. Geophys. Res.*, *88*, 10809-10817, 1983.

Hudson, R. D., and L. J. Kieffer, *Absorption Cross Sections of Stratospheric Molecules, The Natural Stratosphere of 1974, CIAP Monogr. 1*, U. S. Department of Transportation, Washington, D. C., 1975.

Hudson, R. D., and E. I. Reed (Eds.), The Stratosphere: Present and Future, *NASA RP 1049*, 1979.

Hudson, R. D., et al. (Ed.), The Stratosphere 1981: Theory and Measurements, *Rep. 11*, Global Ozone Res. Monit. Proj., World Meteorol. Org., Geneva, 1982.

Inn, E. Ç. Y., Absorption coefficient of *HCl* in the region 1400 to 2200 Å, *J. Atmos. Sci.*, *32*, 2375-2377, 1975.

Isaksen, I. S. A., K. H. Midtbo, J. Sunde, and P. J. Crutzen, A simplified method to include molecular scattering and reflection in calculations of photon fluxes and photodissociation rates, *Geophys. Norv.*, *31*, 11-26, 1977.

Johnston, H. S., Global ozone balance in the natural stratosphere, *Rev. Geophys. 13*, 637-649, 1975.

Johnston, H. S., and J. Podolske, Interpretation of stratospheric photochemistry, *Rev. Geophys.*, *16*, 491-519, 1978.

Johnston, H. S., M. Paige, and F. Yao, Oxygen absorption cross sections in the Herzberg continuum and between 206 and 327 K, *J. Geophys. Res.*, *89*, 11,661-11,665, 1984.

Kaufman, F., L. X. Qiu, and U. C. Sridharan, Radical-radical and atom-radical reactions of HO_2, paper presented at 7th International Symposium on Gas Kinetics, Göttingen, Federal Republic of Germany, August 23-27, 1982.

Keyser, L. F., Kinetics of the reaction $O + HO_2 \rightarrow OH + O_2$ from 229 to 372 K, *J. Phys. Chem.*, *86*, 3439-3446, 1982.

Keyser, L. F., High-pressure flow kinetics, A study of the OH + *HCl* reaction from 2 to 100 Torr, *J. Phys. Chem.*, *88*, 4750-4758, 1984.

Kircher, C. C., and S. P. Sander, Kinetics and mechanism of HO_2 and DO_2 disproportionations, *J. Phys. Chem.*, *88*, 2082-2091, 1984.

Ko, M. K. W., and N. D. Sze, Effect of recent rate data revisions on stratospheric modeling, *Geophys. Res. Lett.*, *10*, 341-344, 1983.

Ko, M. K. W., and N. D. Sze, Diurnal variation of *ClO*: Implications for the stratospheric chemistries of $ClONO_2$, *HOCl*, and *HCl*, *J. Geophys. Res.*, *89*, 11,619-11,632, 1984.

Kramer, R. F., and G. F. Widhopf, Evaluation of daylight or diurnally averaged photolytic rate coefficients in atmospheric photochemical models, *J. Atmos. Sci.*, *35*, 1726-1734, 1978.

Krueger, A. J., The mean ozone distribution from several series of rocket soundings to 52 km at latitudes from 48°S to 64°N, *Pure Appl. Geophys.*, *106-108*, 1272-1280, 1973.

Krueger, A. J., and R. A. Minzner, A mid-latitude ozone model for the 1976 U.S. Standard Atmosphere, *J. Geophys. Res.*, *81*, 4477-4481, 1976.

Krueger, A. J., B. Guenther, A. J. Fleig, D. F. Heath, E. Hilsenrath, R. McPeters, and C. Prabhakara, Satellite ozone measurements, *Phil. Trans. R. Soc. London, Ser. A*, *296*, 191-204, 1980.

Kurzeja, R. J., The diurnal variation of minor constituents in the stratosphere and its effect on the ozone concentration, *J. Atmos. Sci.*, *32*, 899-909, 1975.

Kurzeja, R. J., Effects of diurnal variations and scattering on ozone in the stratosphere for present-day and predicted future chlorine concentrations, *J. Atmos. Sci.*, *34*, 1120-1129, 1977.

Langhoff, S. R., R. L. Jaffe, and J. O. Arnold, Effective cross sections and rate constants for predissociation of *ClO* in the earth's atmosphere, *J. Quant. Spectrosc. Radiat. Transfer*, *18*, 227-235, 1977.

Lean, J. L., Observation of the diurnal variation of atmospheric ozone, *J. Geophys. Res.*, *87*, 4973-4980, 1982.

Lean, J. L., O. R. White, W. C. Livingston, D. F. Heath, R. F. Donnelly, and A. Skumanich, A three-component model of the variability of the solar ultraviolet flux: 145-200 nm, *J. Geophys. Res.*, *87*, 10307-10317, 1982.

Leifer, R., K. Sommers, and S. F. Guggenheim, Atmospheric trace gas measurements with a new clean air sampling system, *Geophys. Res. Lett.*, *8*, 1079-1081, 1981.

Leu, M. T., Kinetics of the reaction O + ClO → Cl + O_2, *J. Phys. Chem.*, *88*, 1394-1398, 1984.

Liu, S. C., M. McFarland, D. Kley, O. Zafiriou, and B. Huebert, Tropospheric NO_x and O_3 budgets in the equatorial Pacific, *J. Geophys. Res.*, *88*, 1360-1368, 1983.

Logan, J. A., M. J. Prather, S. C. Wofsy, and M. B. McElroy, Atmospheric chemistry: Response to human influence, *Phil. Trans. R. Soc. London, Ser. A*, *290*, 187-234, 1978.

Logan, J. A., M. J. Prather, S. C. Wofsy, and M. B. McElroy, Tropospheric chemistry: A global perspective, *J. Geophys. Res.*, *86*, 7210-7254, 1981.

London, J., J. E. Frederick, and G. P. Anderson, Satellite observations of the global distribution of stratospheric ozone, *J. Geophys. Res.*, *82*, 2543-2556, 1977.

Luther, F. M., and R. J. Gelinas, Effect of molecular multiple scattering and surface albedo on atmospheric photodissociation rates, *J. Geophys. Res.*, *81*, 1125-1132, 1976.

Luther, F. M., D. J. Wuebbles, W. H. Duewer, and J. S. Chang, Effect of multiple scattering on species concentrations and model sensitivity, *J. Geophys. Res.*, *83*, 3563-3570, 1978.

Magnotta, F., and H. S. Johnston, Photodissociation quantum yields for the NO_3 free radical, *Geophys. Res. Lett.*, *7*, 769-772, 1980.

Margitan, J. J., Chlorine nitrate: The sole product of the ClO + NO_2 + M recombination, *J. Geophys. Res.*, *88*, 5416-5420, 1983.

Margitan, J. J., Kinetics of the reaction O + ClO → Cl + O_2, *J. Phys. Chem.*, *88*, 3638-3643, 1984.

Martin, B., Accuracy of some methods for determining photodissociation rates in the modeling of stratospheric ozone, *J. Atmos. Sci.*, *33*, 131-134, 1976.

Massie, S. T., and D. M. Hunten, Stratospheric eddy diffusion coefficients from tracer data, *J. Geophys. Res.*, *86*, 9859-9868, 1981.

Mauersberger, K., R. Finstad, S. Anderson, and D. Robbins, A comparison of ozone measurements, *Geophys. Res. Lett.*, *8*, 361-364, 1981.

McPeters, R. D., The behavior of ozone near the stratopause from two years of BUV observations, *J. Geophys. Res.*, *85*, 4545-4550, 1980.

McPeters, R. D., D. F. Heath, and P. K. Bhartia, Average ozone profile for 1979 from the NIMBUS 7 SBUV instrument, *J. Geophys. Res.*, *89*, 5199-5214, 1984.

Meier, R. R., D. E. Anderson, Jr., and M. Nicolet, Radiation field in the troposphere and stratosphere from 240-1000 nm, 1, General analysis, *Planet. Space Sci.*, *30*, 923-933, 1982.

Menzies, R. T., Remote measurement of ClO in the stratosphere, *Geophys. Res. Lett.*, *6*, 151-154, 1979.

Menzies, R. T., A reevaluation of laser heterodyne radiometer ClO measurements, *Geophys. Res. Lett.*, *10*, 729-732, 1983.

Mihelcic, D., D. H. Ehhalt, G. F. Kulessa, J. Klomfass, M. Trainer, U. Schmidt, and H. Rohrs, Measurements of free radicals in the atmosphere by matrix isolation and electron paramagnetic resonance, *Pure Appl. Geophys.*, *116*, 530-536, 1978.

Molina, M. J., and F. S. Rowland, Stratospheric sink for chlorofluoromethanes: Chlorine atom catalyzed destruction of ozone, *Nature*, *249*, 810-812, 1974.

Molina, M. J., L. T. Molina, and C. A. Smith, The rate of the reaction of OH with HCl, *Int. J. Chem. Kinet.*, *16*, 1151-1160, 1984.

Mount, G. H., and G. J. Rottman, The solar spectral irradiance 1200-3184 Å near solar maximum: July 15, 1980, *J. Geophys. Res.*, *86*, 9193-9198, 1981.

Mount, G. H., and G. J. Rottman, The solar absolute spectral irradiance 1150-3173 Å May 17, 1982, *J. Geophys. Res.*, *88*, 5403-5410, 1983.

Mount, G. H., G. J. Rottman, and J. G. Timothy, The solar spectral irradiance 1200-2550 Å at solar maximum, *J. Geophys. Res.*, *85*, 4271-4274, 1980.

Mumma, M. J., J. D. Rogers, T. Kostiuk, D. Deming, J. J. Hillman, and D. Zipoy, Is there any chlorine monoxide in the stratosphere?, *Science*, *221*, 268-271, 1983.

Murcray, D. G., A. Goldman, F. H. Murcray, F. J. Murcray, and W. J. Williams, Stratospheric distribution of $ClONO_2$, *Geophys. Res. Lett.*, *6*, 857-859, 1979.

Myer, J. A., and J. A. R. Samson, Vacuum-ultraviolet absorption cross sections of CO, HCl, and ICN between 1050 and 2100 Å, *J. Chem. Phys.*, *52*, 266-271, 1970.

Nagatani, R. M., and A. J. Miller, Stratospheric ozone changes during the first year of SBUV observations, *J. Geophys. Res.*, *89*, 5191-5198, 1984.

Nicolet, M., Stratospheric ozone: An introduction to its study, *Rev. Geophys.*, *13*, 593-636, 1975*a*.

Nicolet, M., On the production of nitric oxide by cosmic rays in the mesosphere and stratosphere, *Planet. Space Sci.*, *23*, 637-649, 1975*b*.

Nicolet, M., *Etude des Reactions Chimiques de l'Ozone dans la Stratosphere*, Comité d'Etudes sur les Consequences des Vols Stratospheriques, Institut Royal Meteorologique de Belgique, Brussels, 1978.

Nicolet, M., R. R. Meier, and D. E. Anderson, Jr., Radiation field in the troposphere and stratosphere, 2, Numerical analysis, *Planet. Space Sci.*, *30*, 935-983, 1982.

Noxon, J. F., W. R. Henderson, and R. B. Norton, Stratospheric NO_2, 3, The effects of large-scale horizontal transport, *J. Geophys. Res.*, *88*, 5240-5248, 1983.

National Research Council, *Causes and Effects of Stratospheric Ozone Reduction: An Update*, National Academy Press, Washington, D.C., 1982.

Ongstad, A. P., and J. W. Birks, Studies of reactions of importance in the stratosphere, V. Rate constants for the reactions O + NO_2 → NO + O_2 and O + ClO → Cl + O_2 at 298 K, *J. Chem. Phys.*, *81*, 3922-3930, 1984.

Parrish, A., R. L. de Zafra, P. M. Solomon, J. W. Barrett, and E. R. Carlson, Chlorine oxide in the stratospheric ozone layer: Ground-based detection and measurement, *Science*, *211*, 1158-1161, 1981.

Patrick, R., and M. J. Pilling, The temperature dependence of the HO_2 + HO_2 reaction, *Chem. Phys. Lett.*, *91*, 343-347, 1982.

Pitari, G., and G. Visconti, A simple method to account for Rayleigh scattering effects on photodissociation rates, *J. Atmos. Sci.*, *36*, 1803-1811, 1979.

Pitts, Jr., J. N., H. L. Sandoval, and R. Atkinson, Relative rate constants for the reaction of $O(^1D)$ atoms with fluorocarbons and N_2O, *Chem. Phys. Lett.*, *29*, 31-34, 1974.

Prasad, S. S., Possible existence and chemistry of $ClOO_2$ in the stratosphere, *Nature*, *285*, 152-154, 1980.

Prather, M. J., Solution of the inhomogeneous Rayleigh scattering atmosphere, *Astrophys. J.*, *192*, 787-792, 1974.

Prather, M. J., Ozone in the upper stratosphere and mesosphere, *J. Geophys. Res.*, *86*, 5325-5338, 1981.

Prather, M. J., M. B. McElroy, and S. C. Wofsy, Reductions in ozone at high concentrations of stratospheric halogens, *Nature*, *312*, 227-231, 1984.

Pyle, J. A., and C. F. Rogers, Stratospheric transport by stationary planetary waves -- the importance of chemical processes, *Q. J. R. Meteorol. Soc.*, *106*, 421-446, 1980.

Rasmussen, R. A., M. A. K. Khalil, A. J. Crawford, and P. J. Fraser, Natural and anthropogenic trace gases in the southern hemisphere, *Geophys. Res. Lett.*, *9*, 704-707, 1982.

Reiter, R., and M. P. McCormick, SAGE-European ozone-sonde comparison, *Nature*, *300*, 337-339, 1982.

Remsberg, E. E., J. M. Russell, III, J. C. Gille, L. L. Gordley, P. L. Bailey, W. G. Planet, and J. E. Harries, The validation of Nimbus 7 LIMS measurements of ozone, *J. Geophys. Res.*, *89*, 5161-5178, 1984.

Rood, R. B. and A. R. Douglass, Interpretation of ozone temperature correlations, *J. Geophys. Res.*, *90*, 5733-5744, 1985.

Rood, R. B., and M. R. Schoeberl, A mechanistic model of Eulerian, Lagrangian mean, and Lagrangian ozone transport by steady planetary waves, *J. Geophys. Res.*, *88*, 5208-5218, 1983.

Roscoe, H. K., J. R. Drummond, and R. F. Jarnot, Infrared measurements of stratospheric composition, 3, The daytime changes of NO and NO_2, *Proc. R. Soc. London, Ser. A*, *375*, 507-528, 1981.

Rottman, G. J., Rocket measurements of the solar spectral irradiance during solar minimum, 1972-1977, *J. Geophys. Res.*, *86*, 6697-6705, 1981.

Rottman, G. J., C. A. Barth, R. J. Thomas, G. H. Mount, G. M. Lawrence, D. W. Rusch, R. W. Sanders, G. E. Thomas, and J. London, Solar spectral irradiance, 120-190 nm, October 13, 1981 to January 3, 1982, *Geophys. Res. Lett.*, *9*, 587-590, 1982.

Rowland, F. S., and M. J. Molina, Chlorofluoromethanes in the environment, *Rev. Geophys.*, *13*, 1-35, 1975.

Rundel, R. D., Determination of diurnal average photodissociation rates, *J. Atmos. Sci.*, *34*, 639-641, 1977.

Rusch, D. W., G. H. Mount, C. A. Barth, G. J. Rottman, R. J. Thomas, G. E. Thomas, R. W. Sanders, G. M. Lawrence, and R. S. Eckman, Ozone densities in the lower mesosphere measured by a limb scanning ultraviolet spectrometer, *Geophys. Res. Lett.*, *10*, 241-244, 1983.

Russell, J. M., III, J. C. Gille, E. E. Remsberg, L. L. Gordley, P. L. Bailey, S. R. Drayson, H. Fischer, A. Girard, J. E. Harries, and W. F. J. Evans, Validation of nitrogen dioxide results measured by the Limb Infrared Monitor of the Stratosphere (LIMS) experiment on Nimbus 7, *J. Geophys. Res.*, *89*, 5099-5107, 1984.

Sander, S. P., and M. E. Peterson, Kinetics of the reaction HO_2 + NO_2 + M → HO_2NO_2 + M, *J. Phys. Chem.*, *88*, 1566-1571, 1984.

Sander, S. P., and R. T. Watson, Kinetics studies of the reactions of CH_3O_2 with NO, NO_2, and CH_3O_2 at 298 K, *J. Phys. Chem.*, *84*, 1664-1674, 1980.

Schwab, J. J., D. W. Toohey, W. H. Brune, and J. G. Anderson, Reaction kinetics of O + *Cl*O → *Cl* + O_2 between 252-347 K, *J. Geophys. Res.*, *89*, 9581-9587, 1984.

Shardanand, and A. D. Prasad Rao, Collision-induced absorption of O_2 in the Herzberg continuum, *J. Quant. Spectrosc. Radiat. Transfer*, *17*, 433-439, 1977.

Solomon, P. M., R. de Zafra, A. Parrish, and J. W. Barrett, Diurnal variation of stratospheric chlorine monoxide: A critical test of chlorine chemistry in the ozone layer, *Science*, *224*, 1210-1214, 1984.

Solomon, S., and R. R. Garcia, On the distribution of nitrogen dioxide in the high-latitude stratosphere, *J. Geophys. Res.*, *88*, 5229-5239, 1983.

Solomon, S., and R. R. Garcia, On the distributions of long-lived tracers and chlorine species in the middle atmosphere, *J. Geophys. Res.*, *89*, 1163-11,644, 1984.

Solomon, S., H. S. Johnston, M. Kowalczyk, and I. Wilson, Instantaneous global ozone balance including observed nitrogen dioxide, *Pure Appl. Geophys.*, *118*, 58-85, 1980.

Solomon, S., D. W. Rusch, R. J. Thomas, and R. S. Eckman, Comparison of mesospheric ozone abundances measured by the Solar Mesosphere Explorer and model calculations, *Geophys. Res. Lett.*, *10*, 249-252, 1983.

Sreedharan, C. R., and A. Mani, Ozone and temperature changes in the lower stratosphere, *Pure Appl. Geophys.*, *106-108*, 1576-1580, 1973.

Sridharan, U. C., L. X. Qiu, and F. Kaufman, Kinetics and product channels of the reactions of HO_2 with O and H atoms at 296 K, *J. Phys. Chem.*, *86*, 4569-4574, 1982.

Sridharan, U. C., L. X. Qiu, and F. Kaufman, Rate constant of the OH + HO_2 reaction from 252 to 420 K, *J. Phys. Chem.*, *88*, 1281-1282, 1984.

Strobel, D. F., Parametrization of linear wave chemical transport in planetary atmospheres by eddy diffusion, *J. Geophys. Res.*, *86*, 9806-9810, 1981.

Sundararaman, N., The UV radiation field in the stratosphere, paper presented at Fourth Conference on Clim. Impact Assessment Program, U.S. Dep. Transp., Washington, D. C., 1975.

Sze, N. D., and M. K. W. Ko, The effects of the rate for OH + HNO_3 and HO_2NO_2 photolysis on the stratospheric chemistry, *Atmos. Environ.*, *15*, 1301-1307, 1981.

Thrush, B. A., and G. S. Tyndall, The rate of reaction between HO_2 radicals at low pressures, *Chem. Phys. Lett.*, *92*, 232-235, 1982.

Turco, R. P., and R. C. Whitten, A note on the diurnal averaging of aeronomical models, *J. Atmos. Terr. Phys.*, *40*, 13-20, 1978.

Vedder, J. F., B. J. Tyson, R. B. Brewer, C. A. Boitnott, and E. C. Y. Inn, Lower stratosphere measurements of variation with latitude of CF_2Cl_2, $CFCl_3$, CCl_4, and N_2O profiles in the northern hemisphere, *Geophys. Res. Lett.*, *5*, 33-36, 1978.

Vedder, J. F., E. C. Y. Inn, B. J. Tyson, C. A. Boitnott, and D. O'Hara, Measurements of CF_2Cl_2, $CFCl_3$, and N_2O in the lower stratosphere between 2°S and 73°N latitude, *J. Geophys. Res.*, *86*, 7363-7368, 1981.

Waters, J. W., J. C. Hardy, R. F. Jarnot, and H. M. Pickett, Chlorine monoxide radical, ozone and hydrogen peroxide: Stratospheric measurements by microwave limb sounding, *Science*, *214*, 61-64, 1981.

Weinstock, E. M., M. J. Phillips, and J. G. Anderson, In situ observations of *Cl*O on the stratosphere: A review of recent results, *J. Geophys. Res.*, *86*, 7273-7278, 1981.

Whitten, R. C., and R. P. Turco, Diurnal variations of HO_x and NO_x in the stratosphere, *J. Geophys. Res.*, *79*, 1302-1304, 1974.

Yoshino, K., D. E. Freedman, J. R. Esmond, and W. H. Parkinson, High resolution absorption cross section measurements and band oscillator strengths of the (1,0)-(12,0) Schumann-Runge bands of O_2, *Planet. Space Sci.*, *31*, 339-353, 1983.

Zellner, R., and V. Handwerk, Kinetics of the reactions of *Cl*O radicals with NO_2 and O_2, paper presented at the International Symposium on Chemical Kinetics Related to Atmospheric Chemistry, Tsukuba, Ibaraki, Japan, June 6-10, 1982.

M. Allen and L. Froidevaux, Jet Propulsion Laboratory, California Institute of Technology, 4800 Oak Grove Drive, Pasadena, CA 91109.

Y. L. Yung, Division of Geological and Planetary Sciences, California Institute of Technology, Pasadena, CA 91125.

(Received August 13, 1984;
revised April 9, 1985;
accepted April 17, 1985.)